On the correlation between continuum mechanics entities and cell activity in biological soft tissues: Assessment of three possible criteria for cell-controlled fibre reorientation in collagen gels and collagenous tissues

Martin Kroon

www.elsevier.com/locate/yjtbi

On the correlation between continuum mechanics entities and cell activity in biological soft tissues: Assessment of three possible criteria for cell-controlled fibre reorientation in collagen gels and collagenous tissues

Martin Kroon

PII: S0022-5193(09)00602-X
DOI: doi:10.1016/j.jtbi.2009.12.029
Reference: YJTBI5819

To appear in: *Journal of Theoretical Biology*

Received date: 26 August 2009
Revised date: 22 December 2009
Accepted date: 24 December 2009

Cite this article as: Martin Kroon, On the correlation between continuum mechanics entities and cell activity in biological soft tissues: Assessment of three possible criteria for cell-controlled fibre reorientation in collagen gels and collagenous tissues, *Journal of Theoretical Biology*, doi:10.1016/j.jtbi.2009.12.029

On the Correlation Between Continuum Mechanics Entities and Cell Activity in Biological Soft Tissues: Assessment of Three Possible Criteria for Cell-controlled Fibre Reorientation in Collagen Gels and Collagenous Tissues

Martin Kroon*

Department of Solid Mechanics,
Royal Institute of Technology,
Osquars backe 1, SE-100 44 Stockholm, Sweden

Abstract

The biomechanical behaviour of biological cells is of great importance in many physiological processes. One such process is the maintenance of fibrous networks, such as collagenous tissues. The activity of the fibre-producing cells in this type of tissue is very important, and a comprehensive material description needs to incorporate the activity of the cells. In biomechanics, continuum mechanics is often employed to describe deforming solids, and modelling can be much simplified if continuum mechanics entities, such as stress and strain, can be correlated with cell activity. To investigate this, a continuum mechanics framework is employed in which remodelling of a collagen gel is modelled. The remodelling is accomplished by fibroblasts, and the activity of the fibroblasts is linked to the continuum mechanics theory. The constitutive model for the collagen fabric is formulated in terms of a strain energy function, which includes a density function describing the distribution of the collagen fibre orientation. This density function evolves according to an evolution law, where fibroblasts reorient fibres towards the direction of increasing Cauchy stress, elastic deformation, or stiffness. The theoretical framework is applied to experimental results from collagen gels, where gels

*Tel: +46-8-7907553, Fax: +46-8-4112418
Email address: martin@hallf.kth.se (Martin Kroon)

have undergone remodelling under both biaxial and uniaxial constraint. The analyses indicated that criteria 1 and 2 (Cauchy stress and elastic deformations) are able to predict the collagen fibre distribution after remodelling, whereas criterion 3 (current stiffness) is not. This conclusion is, however, tentative and pertains, strictly speaking, only to fibre remodelling processes, and may not be valid for other types of cell activities.

Key words: biomechanics, collagen, collagenous tissues, collagen gel, fibroblast, remodelling

---

1. Introduction

The biological cell constitutes the basic unit of life, and the biomechanical behaviour of cells is of great importance in several physiological processes (Bao and Suresh, 2003; Zhu et al., 2000). The mechanobiology of cells, such as fibroblasts, has therefore been much studied over the last two decades, see e.g. Albrecht-Buehler (1987); Evans and Yeung (1989); Gardel et al. (2003); Heidemann et al. (1999); Hinz and Gabbiani (2003). The fibroblast belongs to the group *adherent* cells, and these cells attach to the extracellular environment (Cukierman et al., 2001; Jiang and Grinnell, 2005). These cells play an important role in the maintenance of the fibrous networks that supply structural integrity to different components of the human body. Collagen is a protein of the human body that supplies structural integrity to such components as bone, cartilage, tendon, skin, and blood vessels. For example, in the wall of blood vessels, collagen acts as a strait-jacket that prohibits acute overdistension of the vessel wall, and collagen can be found in all three layers of the wall (intima, media, and adventitia). The major fibrillar collagens in the vasculature are types I and III. Type I forms thick bundles of fibres, whilst type III forms finer, more reticulate fibres. Both types, synthesised by fibroblasts and smooth muscle cells in the vessel wall, may co-exist within bundles of fibres (Bishop and Lindahl, 1999).

Collagenous tissues are living structures, in which new material may be added and the structural organisation may change over time. The maintenance of the collagen matrix is accomplished by fibre-producing cells, such as fibroblasts. During maintenance, the extracellular matrix (ECM) influences the development, shape, migration, proliferation, survival, and function of the cells. The mobility of the fibroblasts and their ability to contract the ECM are important properties for a proper maintenance of the ECM (En-

gler et al., 2004; Friedl and Bröcker, 2000; Friedrichs et al., 2007; Grinnell, 2003; Lo et al., 2000; Poole et al., 2005). The fibroblast also has the ability to align itself in the direction of existing collagen fibres/fibrils and to produce new collagen that is aligned in the same direction (Birk et al., 1990; Cisneros et al., 2006; Huang et al., 1993; Lin et al., 1999; Meshel et al., 2005; Tóth et al., 1998). Hence, the activity of adherent cells, such as the fibroblast, is strongly dependent upon mechanical stimuli from the surrounding ECM.

The purpose of the present paper is to shed some more light on the interaction between the ECM and the fibre-producing cells. It is well established, that the ECM influences the cell activity, but it is still an open issue how this is done and whether or not continuum mechanics entities, such as stress and strain, can be correlated with cell activity (cf. Humphrey, 2001). To investigate this, we adopt a continuum mechanics description of a collagen gel with embedded fibroblasts. The fibroblasts remodel the collagen gel by reorienting the individual collagen fibres. This reorientation of fibres is described by an evolution law, which depends on a continuum mechanics entity. Three possible choices are assessed: the Cauchy stress, the elastic stretches, and the current stiffness of the material. The three different criteria are evaluated in terms of the predicted distribution of collagen fibres after remodelling, and the outcome is compared to experimental results. Results from tissue equivalents in the form of collagen gels are used when assessing the three criteria.

The continuum mechanics framework and the constitutive model for the collagen gel are outlined in Section 2. The predicted fibre distributions resulting from the three different criteria are compared to experimental results from tests on collagen gels. In Section 3, the proposed model is put on a form that corresponds to the experimental method. A comparison with the experimental results and an evaluation of the three proposed remodelling criteria are provided in Section 4. The results are then discussed in Section 5.

2. Theoretical framework

2.1. Continuum mechanics framework

We consider a network of collagen fibres, where the fibres are embedded in a matrix fluid. The collagen fabric and the surrounding fluid are assumed to be the only load-carrying constituents in the material. Embedded in and attached to the collagen fabric is also a population of fibroblasts. The collagen fabric is composed of collagen *fibres*, which in turn are bundles of collagen

fibrils. The matrix fluid acts as the physiological environment of the collagen and the cells, and the fluid constitutes a continuum in which the collagen fabric is embedded. The fluid does not supply any shear stiffness to the material, but may add a hydrostatic stress component. The deformation of the collagen/fluid matrix is illustrated in Fig. 1, where a reference coordinate system with basis vectors $\mathbf{e}_1$, $\mathbf{e}_2$, $\mathbf{e}_3$ has been introduced. The position vector in the reference configuration Ω_0 is denoted $\mathbf{X} = X_i\mathbf{e}_i$, where X_1, X_2, X_3 are coordinates in the reference system. In a similar way, the position vector in the deformed (current) configuration is denoted $\mathbf{x} = x_i\mathbf{e}_i$. The deformation of a line element in the matrix is described by the deformation gradient $\mathbf{F}(\mathbf{X}) = \partial\mathbf{x}/\partial\mathbf{X}$, which is decomposed according to (cf. Rodriguez et al., 1994)

$$\mathbf{F} = \mathbf{F}_{\mathrm{el}}\mathbf{F}_{\mathrm{lf}}\mathbf{F}_{\mathrm{r}}. \tag{1}$$

The fibroblasts' remodelling of the collagen fabric results in a new matrix configuration Ω_{r}. This deformation of the matrix is described by $\mathbf{F}_{\mathrm{r}}$. The configuration Ω_{r} does not necessarily fulfil equilibrium, and the deformation gradient $\mathbf{F}_{\mathrm{lf}}$ takes the matrix to the state Ω_{lf}, that fulfils global equilibrium with no external loads applied. Finally, if external loads are applied to the material, the configuration Ω_{el} is attained, and this deformation is described by the deformation gradient $\mathbf{F}_{\mathrm{el}}$.

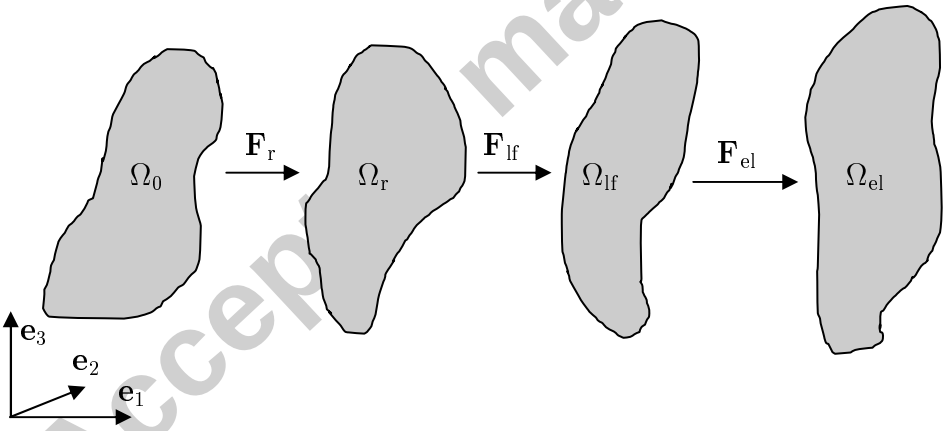

Figure 1: Deformation of physiological matrix in which the collagen fibres and fibroblasts are embedded. Deformation gradients $\mathbf{F}_{\mathrm{r}}$, $\mathbf{F}_{\mathrm{lf}}$, and $\mathbf{F}_{\mathrm{el}}$ describe the deformation of a line element between configurations Ω_0, Ω_{r}, Ω_{lf}, and Ω_{el}, respectively.

The right and left Cauchy-Green deformation tensors are defined as $\mathbf{C} =$

$\mathbf{F}^{\mathrm{T}}\mathbf{F}$ and $\mathbf{b} = \mathbf{F}\mathbf{F}^{\mathrm{T}}$, respectively. The remodelling deformation gradient $\mathbf{F}_{\mathrm{r}}$ is taken to be fully in-elastic, and the total elastic deformation imposed on the matrix is therefore $\mathbf{F}_{\mathrm{e}} = \mathbf{F}_{\mathrm{el}}\mathbf{F}_{\mathrm{lf}}$. The associated right and left Cauchy-Green deformation tensors are $\mathbf{C}_{\mathrm{e}} = \mathbf{F}_{\mathrm{e}}^{\mathrm{T}}\mathbf{F}_{\mathrm{e}} = \mathbf{F}_{\mathrm{r}}^{-\mathrm{T}}\mathbf{C}\mathbf{F}_{\mathrm{r}}^{-1}$ and $\mathbf{b}_{\mathrm{e}} = \mathbf{F}_{\mathrm{e}}\mathbf{F}_{\mathrm{e}}^{\mathrm{T}} = \mathbf{F}\mathbf{F}_{\mathrm{r}}^{-1}\mathbf{F}_{\mathrm{r}}^{-\mathrm{T}}\mathbf{F}^{\mathrm{T}}$. Let $\mathbf{M}$ be a unit vector defined in the reference configuration Ω_0, and let $\mathbf{m} = \mathbf{F}\mathbf{M}/|\mathbf{F}\mathbf{M}|$ be the associated mapped unit vector in the current configuration. We also introduce two sets of spherical coordinates, $\{\theta, \phi\}$ and $\{\theta_{\mathrm{c}}, \phi_{\mathrm{c}}\}$, defined in the reference and current configurations, respectively, such that the unit vectors may be expressed as

$$\mathbf{M} = \sin\theta\cos\phi\mathbf{e}_1 + \sin\theta\sin\phi\mathbf{e}_2 + \cos\theta\mathbf{e}_3 \tag{2}$$

and

$$\mathbf{m} = \sin\theta_{\mathrm{c}}\cos\phi_{\mathrm{c}}\mathbf{e}_1 + \sin\theta_{\mathrm{c}}\sin\phi_{\mathrm{c}}\mathbf{e}_2 + \cos\theta_{\mathrm{c}}\mathbf{e}_3. \tag{3}$$

The elastic stretch $\lambda_{\mathrm{e,m}}$ in the direction $\mathbf{m}$ may be computed as

$$\lambda_{\mathrm{e,m}}^2 = \mathbf{m}\mathbf{b}_{\mathrm{e}}\mathbf{m}. \tag{4}$$

Under physiological conditions, collagenous tissues can be modelled as a hyperelastic material, where the constitutive response is governed by a strain-energy function Ψ. The second Piola-Kirchhoff stress $\mathbf{S}$ is then defined as

$$\mathbf{S} = 2\frac{\partial\Psi}{\partial\mathbf{C}_{\mathrm{e}}}. \tag{5}$$

The first Piola-Kirchhoff stress tensor $\mathbf{P}$ is obtained as $\mathbf{P} = \mathbf{F}_{\mathrm{e}}\mathbf{S}$, and the Cauchy stress $\boldsymbol{\sigma}$ as $\boldsymbol{\sigma} = \mathbf{P}\mathbf{F}_{\mathrm{e}}^{\mathrm{T}}/J_{\mathrm{e}} = \mathbf{F}_{\mathrm{e}}\mathbf{S}\mathbf{F}_{\mathrm{e}}^{\mathrm{T}}/J_{\mathrm{e}}$, where $J_{\mathrm{e}} = \det\mathbf{F}_{\mathrm{e}}$. The normal stress in a direction $\mathbf{m}$ ($|\mathbf{m}| = 1$) is obtained as

$$\sigma_{\mathrm{m}} = \mathbf{m}\boldsymbol{\sigma}\mathbf{m}. \tag{6}$$

The components of the material stiffness tensor $\mathbb{C}_{ijkl}$ are defined as

$$\mathbb{C}_{ijkl} = 2\frac{\partial S_{ij}}{\partial C_{\mathrm{e},kl}}, \tag{7}$$

and from $\mathbb{C}_{ijkl}$ the components of the stiffness tensor in the current configuration $\mathbb{c}_{ijkl}$ are obtained as

$$\mathbb{c}_{ijkl} = F_{\mathrm{e},im}F_{\mathrm{e},jn}F_{\mathrm{e},ko}F_{\mathrm{e},lp}\mathbb{C}_{mnop}. \tag{8}$$

From Eq. (8), the normal stiffness $\mathbb{c}_{\mathrm{m}}$ in a direction $\mathbf{m}$ ($|\mathbf{m}| = 1$) in the current configuration is computed as

$$\mathbb{c}_{\mathrm{m}} = m_i m_j m_k m_l \mathbb{C}_{ijkl}. \tag{9}$$

2.2. Remodelling of collagen network

Remodelling of the collagen fabric implies a restructuring/reorganisation of existing collagen. During maintenance of the collagen fabric, fibroblasts are assumed to remodel the collagen in two different ways: by contracting the collagen network inelastically and by changing the orientation of the fibres.

The density and orientation distribution of fibres are modelled by use of a density function $\rho = \rho(\mathbf{M})$, defined in the reference configuration Ω_0, where $\mathbf{M}$ is defined over the domain Ω_{M}. Thus, $\rho(\mathbf{M})$ gives the density of fibres oriented in a direction defined by the unit vector $\mathbf{M}$, and ρ has the unit kg/m^3. In the current, deformed configuration, the associated distribution is $\rho_{\mathrm{c}}(\mathbf{m})$. We also introduce the volume concentration of fibroblasts, ρ_{f} and $\rho_{\mathrm{f,c}}$, defined in the reference and current configurations, respectively, where both ρ_{f} and $\rho_{\mathrm{f,c}}$ have the unit cells/m^3.

The first way in which remodelling occurs (the inelastic contraction) is conjectured to take place in the following way: a) a collagen fibre is removed from the network by a fibroblast, (b) the fibroblast then contracts the remaining network of fibres, and c) the fibroblast reinserts the released fibre. This process is modelled by the tensor $\mathbf{F}_{\mathrm{r}}$. The right Cauchy-Green deformation tensor $\mathbf{C}_{\mathrm{r}} = \mathbf{F}_{\mathrm{r}}^{\mathrm{T}}\mathbf{F}_{\mathrm{r}}$ is completely defined in the reference configuration, and the evolution of the remodelling process may be modelled by use of the rate

$$\begin{aligned}\dot{\mathbf{C}}_{\mathrm{r}} &= \frac{\mathrm{d}}{\mathrm{d}t}\sum_{i=1}^{3}\lambda_{\mathrm{r},i}^2\widehat{\mathbf{N}}_{\mathrm{r},i}\otimes\widehat{\mathbf{N}}_{\mathrm{r},i} = \\ &= \sum_{i=1}^{3}\left(\dot{\overline{\lambda_{\mathrm{r},i}^2}}\widehat{\mathbf{N}}_{\mathrm{r},i}\otimes\widehat{\mathbf{N}}_{\mathrm{r},i} + \lambda_{\mathrm{r},i}^2\dot{\widehat{\mathbf{N}}}_{\mathrm{r},i}\otimes\widehat{\mathbf{N}}_{\mathrm{r},i} + \lambda_{\mathrm{r},i}^2\widehat{\mathbf{N}}_{\mathrm{r},i}\otimes\dot{\widehat{\mathbf{N}}}_{\mathrm{r},i}\right), \qquad (10)\end{aligned}$$

where $\lambda_{\mathrm{r},i}$ are the principal stretches of $\mathbf{F}_{\mathrm{r}}$, and $\widehat{\mathbf{N}}_{\mathrm{r},i}$ are the principal directions of $\mathbf{C}_{\mathrm{r}}$. Evolution laws for $\lambda_{\mathrm{r},i}$ and $\widehat{\mathbf{N}}_{\mathrm{r},i}$ are required and may be formulated as

$$\dot{\overline{\lambda_{\mathrm{r},i}^2}} = \dot{\overline{\lambda_{\mathrm{r},i}^2}}(\mathbf{F}, \mathbf{F}_{\mathrm{r}}, \boldsymbol{\sigma}, \dots), \qquad (11)$$

$$\dot{\widehat{\mathbf{N}}}_{\mathrm{r},i} = \dot{\widehat{\mathbf{N}}}_{\mathrm{r},i}(\mathbf{F}, \mathbf{F}_{\mathrm{r}}, \boldsymbol{\sigma}, \dots), \qquad (12)$$

i.e. the evolution laws can be expected to depend on the deformation gradients $\mathbf{F}$ and $\mathbf{F}_{\mathrm{r}}$, the Cauchy stress tensor $\boldsymbol{\sigma}$, and possibly other entities.

The second way that fibroblasts remodel the collagen network is by reorienting fibres, which is modelled by a diffusion-like evolution law according to

$$\frac{\partial \rho_{\mathrm{c}}(\mathbf{m})}{\partial t} + \beta \rho_{\mathrm{f,c}} \rho_{\mathrm{c}}(\mathbf{m}) \Delta q(\mathbf{m}) = \dot{m}(\mathbf{m}), \tag{13}$$

where the entities $\rho_{\mathrm{c}}(\mathbf{m})$, $\rho_{\mathrm{f,c}}$, $q(\mathbf{m})$, $\dot{m}(\mathbf{m})$, and $\mathbf{m}$ are defined in the current configuration. Thus, $\rho(\mathbf{M})$ in the reference configuration is mapped to $\rho_{\mathrm{c}}(\mathbf{m})$ in the current configuration, β (with the unit $\mathrm{m}^3/(\mathrm{cells}{\cdot}\mathrm{s}{\cdot}\mathrm{Pa})$) is a material constant, q is a continuum mechanics entity to be specified below, $\dot{m}$ is the collagen mass production rate per unit deformed volume, and t denotes time. No material growth is included in the present model, and the mass production rate is therefore zero, i.e. $\dot{m}(\mathbf{m}) \equiv 0$.

If $\mathbf{m}$ is expressed in terms of the spherical coordinates introduced in Eq. (3), the derivative in the second term of Eq. (13) takes on the form

$$\Delta q = \frac{1}{\sin\theta_{\mathrm{c}}} \frac{\partial}{\partial \theta_{\mathrm{c}}} \left(\sin\theta_{\mathrm{c}} \frac{\partial q}{\partial \theta_{\mathrm{c}}} \right) + \frac{1}{\sin^2\theta_{\mathrm{c}}} \frac{\partial^2 q}{\partial \phi_{\mathrm{c}}^2}. \tag{14}$$

Three possible choices of q will be explored in the present analysis:

- $q_1 = \sigma_{\mathrm{m}}$ (the normal stress in Eq. (6)),
- $q_2 = \lambda_{\mathrm{m}}^2$ (the normal elastic deformation in Eq. (4)),
- $q_3 = \mathbb{C}_{\mathrm{m}}$ (the normal stiffness in Eq. (9)).

Criteria 1, 2, and 3 imply that fibroblasts reorient collagen fibres towards the direction of increasing stress, elastic deformation, and stiffness, respectively.

2.3. Strain energy function for collagen network

On the macroscopic level, collagen fabrics display a non-linear stress-strain behaviour, which is related to geometric characteristics, i.e. the waviness of the collagen fibrils. Both phenomenological and microstructurally based approaches have been used when deriving constitutive models for collagen. Diamant et al. (1972) modelled a single collagen fibre as a linear elastic zig-zag wave with rigid nodes. Other studies have treated collagen fibrils as planar, sinusoidal-like, slender filaments, e.g. Buckley et al. (1980); Comninou and Yannas (1976); Hurschler et al. (1997); Lanir (1978, 1979b). A more advanced approach was chosen by Annovazzi and Genna (2009), who

considered a collagen fibre unit as being composed of a parallel arrangement of subunits down to the tropocollagen level.

Phenomenological models, on the other hand, are plausible mathematical expressions that are able to fit experimental stress-strain relations, but lack a clear microstructural motivation. Fung (1967) proposed a phenomenological constitutive model for collagenous tissues, and several other functional forms have followed. Uniaxially oriented collagen may, due to its waviness (or undulation), be described by a strain energy function on the form

$$\Psi_{\mathrm{c}} = k_{\mathrm{c}}' \left\{ \exp\left(a \left(\lambda_{\mathrm{c}}^2 - 1 \right)^2 \right) - 1 \right\}, \tag{15}$$

where k_{c}' and a are stiffness parameters, and λ_{c} is the stretch imposed on the collagen fibres.

We now consider a network of collagen fibres, having a volume density $\rho(\mathbf{M})$ and deforming affinely with the matrix. External (tensile) loads or constraints are applied, and remodelling occurs in a deformed state $\Omega_{\mathrm{el}} = \Omega_{\mathrm{c}}$. Fig. 2(a) shows the relevant configurations during remodelling under externally imposed loads and/or constraints. In Fig. 2(a), the remodelling is symbolised by a relative sliding between cross-linked collagen fibres and an associated adjustment of the cross-link site (the black dots). To comply with the imposed external boundary conditions, the network also needs to deform elastically, which is described by $\mathbf{F}_{\mathrm{e}}$. The total deformation gradient, associated with the state $\Omega_{\mathrm{el}} = \Omega_{\mathrm{c}}$ is $\mathbf{F} = \mathbf{F}_{\mathrm{c}}$, and the right Cauchy-Green deformation tensor $\mathbf{C}_{\mathrm{c}} = \mathbf{F}_{\mathrm{c}}^{\mathrm{T}} \mathbf{F}_{\mathrm{c}}$. The elastic deformation, experienced by the fibres in this state, is described by the right Cauchy-Green deformation tensor $\mathbf{C}_{\mathrm{c,e}} = \mathbf{F}_{\mathrm{r}}^{-\mathrm{T}} \mathbf{C}_{\mathrm{c}} \mathbf{F}_{\mathrm{r}}^{-1}$. If the external loads and constraints are removed, the collagen fibres will try to contract the network back to the load-free state of the individual collagen fibres. But the fact that the fibres are intermingled and cross-linked prohibits them from reaching their fully relaxed state. This is illustrated in Fig. 2(b). Hence, the (macroscopically) load-free state Ω_{lf} is not identical to Ω_{r}, and in Ω_{lf}, individual collagen fibres may be in a state of *pre-stretch*. This internal resistance to compression, caused by the interactions between fibres in the network (and possibly other matrix substances), is modelled by introducing a network compression modulus k_{cn} (index "cn" for *collagen network*). We assume that the external loads and constraints change slowly compared to the remodelling process, i.e. $\mathbf{F}_{\mathrm{c}}$ changes slowly compared

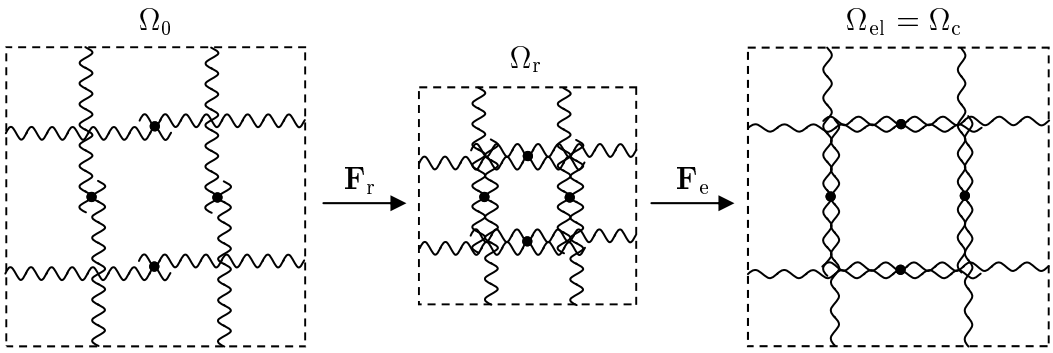

(a) Configurations during remodelling

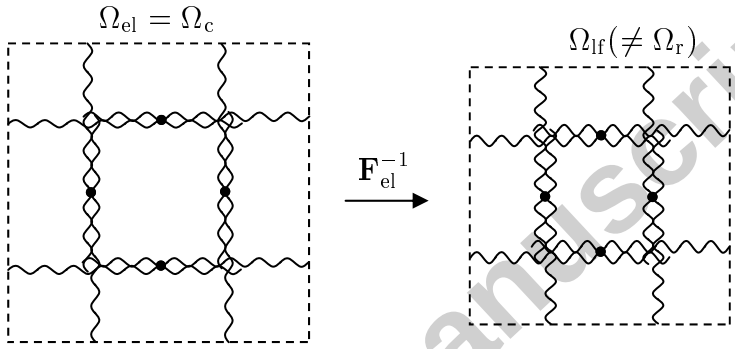

(b) Unloading to load-free state

Figure 2: (a) Configurations during remodelling with external loads and/or constraints applied. Remodelling occurs in the deformed state $\Omega_{el} = \Omega_c$. (b) Unloading from deformed state $\Omega_{el} = \Omega_c$ to load-free state Ω_{lf}.

to $\mathbf{F}_r$. The total strain energy of the collagen network is now modelled as

$$\begin{aligned}\Psi &= \int_{\Omega_M} \rho(\mathbf{M}) \frac{k_c}{4a} \left\{ \exp\left[a\,(\xi-1)^2\right] - 1 \right\} \cdot H(\xi-1) \mathrm{d}\Omega_M \\ &+ \int_{\Omega_M} \rho(\mathbf{M}) \frac{k_{cn}}{4} (\xi_c - \xi)^2 \cdot H(\xi_c - \xi) \mathrm{d}\Omega_M, \qquad (16) \\ &\xi(\mathbf{C}_e, \mathbf{F}_r, \mathbf{M}) = \mathbf{C}_e : \mathbf{A}(\mathbf{F}_r, \mathbf{M}), \\ &\xi_c(\mathbf{C}_{c,e}, \mathbf{F}_r, \mathbf{M}) = \mathbf{C}_{c,e} : \mathbf{A}(\mathbf{F}_r, \mathbf{M}),\end{aligned}$$

where Ω_M is the surface domain over which the density function $\rho(\mathbf{M})$ is defined (typically a half unit sphere), H is the Heaviside step function, and

$\mathbf{A} = \mathbf{F}_{\mathrm{r}}\mathbf{M}/\left|\mathbf{F}_{\mathrm{r}}\mathbf{M}\right| \otimes \mathbf{F}_{\mathrm{r}}\mathbf{M}/\left|\mathbf{F}_{\mathrm{r}}\mathbf{M}\right|$. Thus, in the first term in Eq. (16), collagen fibres in tension ($\xi > 1$) contribute to the strain energy through the exponential-type of law given in Eq. (15). The second term in Eq. (16) accounts for the resistance to network compression, where the compression resistance kicks in when the network is compressed compared to the deformation state in which remodelling has taken place ($\xi < \xi_{\mathrm{c}}$).

3. Model formulation corresponding to experimental method

3.1. Experimental method

The theoretical model proposed in the previous section is applied to experimental results presented by Thomopoulos et al. (2007). Thomopoulos et al. study the mechanical and histological properties of remodelling collagen gels. Collagen gels were created by polymerisation of monomeric bovine type I collagen. Rat cardiac fibroblasts were inserted into the gels. A principle sketch of the experimental set-up is shown in Fig. 3, where basis vectors $\mathbf{e}_1$, $\mathbf{e}_2$, $\mathbf{e}_3$ are indicated. Gels were constrained either uniaxially ($\mathbf{e}_1$-direction) or biaxially ($\mathbf{e}_1$- and $\mathbf{e}_2$-directions) for 72h, during which time the fibroblasts were allowed to remodel the collagen gel. After that, the collagen fibre distribution in the gels was examined by use of a microscope, and the mechanical properties were investigated in terms of equibiaxial, load-controlled tensile tests. In total, 36 gels were investigated by Thomopoulos et al., and the experimental results reproduced below are average values.

3.2. Model prerequisites and kinematics

The collagen gel is idealised as a planar network of collagen fibres embedded in water, and all collagen fibres are thus assumed to lie in the $\mathbf{e}_1$-$\mathbf{e}_2$-plane during testing. The initial distribution of fibres is assumed to be uniform, i.e. fibres have no preferred direction and are perfectly randomly oriented in the $\mathbf{e}_1$-$\mathbf{e}_2$-plane. In Fig. 3, the collagen gel is illustrated together with the basis vectors. Thomopoulos et al. conclude that during the remodelling process, only a minimal amount of additional matrix components was added by the cells. The collagen mass can therefore be taken to be constant.

Since the stresses in the remodelling gels can be expected to be relatively low, we assume that the evolution laws in Eqs. (11) and (12) are independent of the stress state. We assume that the remodelling occurs uniformly in the $\mathbf{e}_1$-$\mathbf{e}_2$-plane and can be described by the tensor

$$\mathbf{F}_{\mathrm{r}} = \lambda_{\mathrm{r}}(\mathbf{e}_1 \otimes \mathbf{e}_1 + \mathbf{e}_2 \otimes \mathbf{e}_2) + \mathbf{e}_3 \otimes \mathbf{e}_3, \tag{17}$$

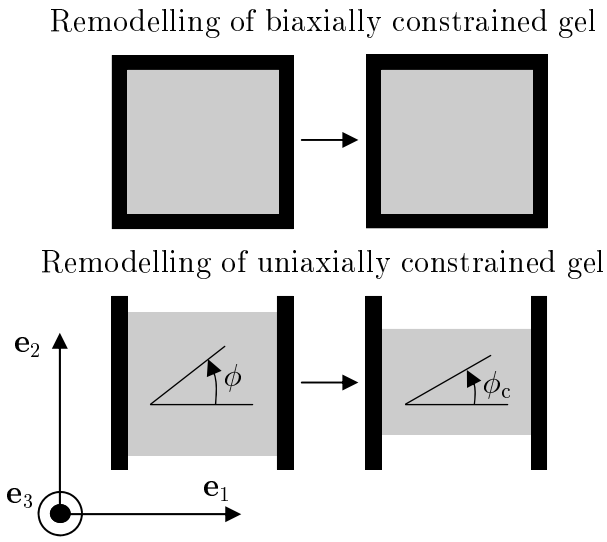

Figure 3: Principle sketch of experimental set-up used by Thomopoulos et al. (2007).

where contraction of the network during remodelling corresponds to $\lambda_r < 1$. Under this assumption, no evolution law for $\widehat{\mathbf{N}}_{r,i}$ is required. For λ_r, we here adopt a phenomenological evolution law on the form

$$\dot{\overline{\lambda_r^2}} = -\alpha \rho_{f,c} J_r^2, \tag{18}$$

where $J_r = \det \mathbf{F}_r = \lambda_r^2$. The material constant α (with the unit $m^3/(\text{cells}\cdot\text{s})$) is related to the reorganisation speed of the fibre-producing cells (such as fibroblasts). Contractions cannot be unbounded, and λ_r should always remain positive. This is ensured by including the factor J_r^2 in Eq. (18). Eq. (18) may be recast into

$$\dot{\lambda}_r = -\frac{\alpha \rho_{f,c} J_r^2}{2\lambda_r}, \tag{19}$$

which defines the evolution law for λ_r.

For the present experimental set-up, homogeneous deformation is assumed and the deformation gradients take on the forms

$$\begin{aligned} \mathbf{F}_r &= \lambda_r(\mathbf{e}_1 \otimes \mathbf{e}_1 + \mathbf{e}_2 \otimes \mathbf{e}_2) + \mathbf{e}_3 \otimes \mathbf{e}_3, \\ \mathbf{F}_e &= \mathbf{F}_{el}\mathbf{F}_{lf} = \lambda_{e,1} \cdot \mathbf{e}_1 \otimes \mathbf{e}_1 + \lambda_{e,2} \cdot \mathbf{e}_2 \otimes \mathbf{e}_2 + \lambda_{e,3} \cdot \mathbf{e}_3 \otimes \mathbf{e}_3, \\ \mathbf{F} &= \mathbf{F}_e\mathbf{F}_r = \lambda_1 \cdot \mathbf{e}_1 \otimes \mathbf{e}_1 + \lambda_2 \cdot \mathbf{e}_2 \otimes \mathbf{e}_2 + \lambda_3 \cdot \mathbf{e}_3 \otimes \mathbf{e}_3, \end{aligned} \tag{20}$$

where $\lambda_1 = \lambda_r\lambda_{e,1}$, $\lambda_2 = \lambda_r\lambda_{e,2}$, and $\lambda_3 = \lambda_{e,3}$. Since the fibres lie in the $\mathbf{e}_1$-$\mathbf{e}_2$-plane, the remodelling process is taken to be confined to this plane, implying $(\mathbf{F}_r)_{33} \equiv 1$. During the elastic deformation $\mathbf{F}_e$, incompressibility is assumed, and the relations $J_e = \det\mathbf{F}_e = \lambda_{e,1}\lambda_{e,2}\lambda_{e,3} = 1$ must therefore hold.

The density function $\rho(\mathbf{M})$ is defined in the $\mathbf{e}_1$-$\mathbf{e}_2$-plane, and the vector $\mathbf{M}$ may be expressed as $\mathbf{M} = \cos\phi\mathbf{e}_1 + \sin\phi\mathbf{e}_2$. Since fibres are taken to remain in the $\mathbf{e}_1$-$\mathbf{e}_2$-plane during deformation in the present experiments, the associated vector $\mathbf{m}$ in the deformed configuration is $\mathbf{m} = \cos\phi_c\mathbf{e}_1 + \sin\phi_c\mathbf{e}_2$, see Fig. 3. The Laplace operator in Eq. (14) simplifies to $\Delta q = \partial^2 q/\partial\phi_c^2$. For this planar type of problem, the current and reference volume densities may be expressed as $\rho(\mathbf{M}) = \rho(\phi)$ and $\rho_c(\mathbf{m}) = \rho_c(\phi_c)$, respectively, and a relation between these entities is required. The deformation gradient $\mathbf{F}_r$ causes an isotropic contraction of the network, resulting in the volume density

$$\rho_r(\phi) = \rho(\phi)/J_r, \tag{21}$$

where $J_r = \det\mathbf{F}_r = \lambda_r^2$. The isochoric elastic deformation $\mathbf{F}_e$ in turn causes a redistribution of the volume density to $\rho_c(\phi_c)$, which may be described by the relation

$$\rho_r(\phi)\mathrm{d}\phi = \rho_c(\phi_c)\mathrm{d}\phi_c. \tag{22}$$

The vectors $\mathbf{M}$ and $\mathbf{m}$ are related as $\mathbf{m} = \mathbf{FM}/|\mathbf{FM}| = \mathbf{F}_e\mathbf{M}/|\mathbf{F}_e\mathbf{M}|$, which after some manipulation gives the relation

$$\lambda_{e,1}\tan\phi_c = \lambda_{e,2}\tan\phi. \tag{23}$$

By differentiating Eq. (23) and combining Eq's. (21)-(23), we obtain the relation

$$\rho_c = \rho_c(\phi, \lambda_{e,1}, \lambda_{e,2}) = \frac{\rho(\phi)}{J_r}\frac{\lambda_{e,1}^2 + \lambda_{e,2}^2\tan^2\phi}{\lambda_{e,1}\lambda_{e,2}(1+\tan^2\phi)}. \tag{24}$$

3.3. Strain energy function, stress and stiffness components

For the 2D collagen network and matrix fluid, the following strain energy function is adopted:

$$\begin{aligned}\Psi = & \int_{\phi=-\pi/2}^{\pi/2} \rho(\phi)\frac{k_c}{4a}\left\{\exp\left[a\left(\xi-1\right)^2\right]-1\right\}\cdot H(\xi-1)\mathrm{d}\phi \\ + & \int_{\phi=-\pi/2}^{\pi/2} \rho(\phi)\frac{k_{cn}}{4}\left(\xi_c-\xi\right)^2\cdot H(\xi_c-\xi)\mathrm{d}\phi \\ + & \frac{k_3}{4}\left(\lambda_{e,3}^2-1\right)^2 - p(J_e-1),\end{aligned} \tag{25}$$

where $\mathbf{C}_\mathrm{e} = \lambda_{\mathrm{e},1}^2 \cdot \mathbf{e}_1 \otimes \mathbf{e}_1 + \lambda_{\mathrm{e},2}^2 \cdot \mathbf{e}_2 \otimes \mathbf{e}_2 + \lambda_{\mathrm{e},3}^2 \cdot \mathbf{e}_3 \otimes \mathbf{e}_3$, $\xi(\mathbf{C}_\mathrm{e}, \mathbf{M}) = \lambda_{\mathrm{e},1}^2 \cos^2\phi + \lambda_{\mathrm{e},2}^2 \sin^2\phi$, and $\xi_\mathrm{c}(\mathbf{C}_{\mathrm{c,e}}, \mathbf{M}) = \lambda_{\mathrm{c,e},1}^2 \cos^2\phi + \lambda_{\mathrm{c,e},2}^2 \sin^2\phi$. Remodelling takes place in a state described by the total deformation gradient $\mathbf{F}_\mathrm{c} = \lambda_{\mathrm{c},1} \cdot \mathbf{e}_1 \otimes \mathbf{e}_1 + \lambda_{\mathrm{c},2} \cdot \mathbf{e}_2 \otimes \mathbf{e}_2 + \lambda_{\mathrm{c},3} \cdot \mathbf{e}_3 \otimes \mathbf{e}_3$. Incompressibility is assumed for the elastic deformation, and p is a Lagrange multiplier that supplies a hydrostatic stress component to the material. As fibres are assumed to be parallel to the $\mathbf{e}_1$-$\mathbf{e}_2$-plane, they do not contribute with any stiffness to the $\mathbf{e}_3$-direction. However, since the fibres are cross-linked, the gel will exhibit a certain stiffness in this direction as well, and a stiffness k_3 (and an associated strain energy term) is therefore assigned to the $\mathbf{e}_3$-direction.

The second Piola-Kirchhoff stress is computed according to Eq. (5), and may, due to the symmetries of the present problem, be expressed as $\mathbf{S} = S_1 \cdot \mathbf{e}_1 \otimes \mathbf{e}_1 + S_2 \cdot \mathbf{e}_2 \otimes \mathbf{e}_2 + S_3 \cdot \mathbf{e}_3 \otimes \mathbf{e}_3$. Plane stress prevails both during the remodelling process and during the equibiaxial tensile tests, and the boundary condition $S_3 = 0$ enables determination of the Lagrange multiplier to $p = k_3 \lambda_{\mathrm{e},3}^2 (\lambda_{\mathrm{e},3}^2 - 1)$. The resulting second Piola-Kirchhoff stress is

$$\begin{aligned} \mathbf{S} &= \int_{\phi=-\pi/2}^{\pi/2} \rho(\phi) k_\mathrm{c} \exp\left[a\left(\xi-1\right)^2\right](\xi-1)\,\mathbf{A} \cdot H(\xi-1)\mathrm{d}\phi \\ &- \int_{\phi=-\pi/2}^{\pi/2} \rho(\phi) k_\mathrm{cn}\left(\xi_\mathrm{c}-\xi\right)\mathbf{A} \cdot H(\xi_\mathrm{c}-\xi)\mathrm{d}\phi \\ &+ k_3\left(\lambda_{e,3}^2-1\right)\mathbf{e}_3 \otimes \mathbf{e}_3 - k_3\lambda_{e,3}^2\left(\lambda_{e,3}^2-1\right)\cdot \mathbf{C}_\mathrm{e}^{-1}, \end{aligned} \tag{26}$$

where $\mathbf{A} = \cos^2\phi \cdot \mathbf{e}_1 \otimes \mathbf{e}_1 + \sin^2\phi \cdot \mathbf{e}_2 \otimes \mathbf{e}_2 + \cos\phi\sin\phi(\mathbf{e}_1 \otimes \mathbf{e}_2 + \mathbf{e}_2 \otimes \mathbf{e}_1)$, and $\lambda_{e,3} = (\lambda_{e,1}\lambda_{e,2})^{-1}$ due to incompressibility. The first Piola-Kirchhoff stress $\mathbf{P}$ and Cauchy stress $\boldsymbol{\sigma}$ are computed as $\mathbf{P} = \mathbf{F}_\mathrm{e}\mathbf{S}$ and $\boldsymbol{\sigma} = \mathbf{P}\mathbf{F}_\mathrm{e}^\mathrm{T}$, and will be on the forms $\mathbf{P} = P_1 \cdot \mathbf{e}_1 \otimes \mathbf{e}_1 + P_2 \cdot \mathbf{e}_2 \otimes \mathbf{e}_2$ and $\boldsymbol{\sigma} = \sigma_1 \cdot \mathbf{e}_1 \otimes \mathbf{e}_1 + \sigma_2 \cdot \mathbf{e}_2 \otimes \mathbf{e}_2$, respectively.

The components of the material stiffness tensor take on the forms ($i, j =$

1, 2)

$$\begin{aligned}\mathbb{C}_{ijkl} &= 2\frac{\partial S_{ij}}{\partial C_{\mathrm{e},kl}} = 2k_{\mathrm{c}}\int_{\phi=-\pi/2}^{\pi/2}\rho(\phi)\exp\left[a\left(\xi-1\right)^2\right]\cdot \\ &\quad \cdot\left\{1+2a\left(\xi-1\right)\right\}\cdot H(\xi-1)A_{ij}A_{kl}\mathrm{d}\phi + \\ &\quad +2k_{\mathrm{cn}}\int_{\phi=-\pi/2}^{\pi/2}\rho(\phi)A_{ij}A_{kl}\cdot H(\xi_{\mathrm{c}}-\xi)\mathrm{d}\phi + \\ &\quad +2k_3\lambda_{e,3}^2\left(2\lambda_{e,3}^2-1\right)\cdot C_{\mathrm{e},ij}^{-1}C_{\mathrm{e},kl}^{-1} + \\ &\quad +k_3\lambda_{e,3}^2\left(\lambda_{e,3}^2-1\right)\cdot(C_{\mathrm{e},ik}^{-1}C_{\mathrm{e},lj}^{-1}+C_{\mathrm{e},il}^{-1}C_{\mathrm{e},kj}^{-1}),\end{aligned} \tag{27}$$

and the components $\mathbb{c}_{ijkl}$ of the current stiffness tensor are then computed according to Eq. (8).

In the evolution law Eq. (13), the entity $\partial^2 q/\partial\phi_{\mathrm{c}}^2$ is required, where three different candidates for q will be explored. In the present problem formulation, q_1, q_2, and q_3 take on the following forms:

$$q_1 = \sigma_{\mathrm{m}} = \sigma_1\cos^2\phi_{\mathrm{c}} + \sigma_2\sin^2\phi_{\mathrm{c}}, \tag{28}$$

$$q_2 = \lambda_{\mathrm{m}}^2 = \lambda_{\mathrm{e},1}^2\cos^2\phi_{\mathrm{c}} + \lambda_{\mathrm{e},2}^2\sin^2\phi_{\mathrm{c}}, \tag{29}$$

$$\begin{aligned}q_3 = \mathbb{C}_{\mathrm{m}} &= b_1\cos^4\phi_{\mathrm{c}} + b_2\cos\phi_{\mathrm{c}}\sin^3\phi_{\mathrm{c}} + b_3\cos^2\phi_{\mathrm{c}}\sin^2\phi_{\mathrm{c}} \\ &+ b_4\cos\phi_{\mathrm{c}}\sin^3\phi_{\mathrm{c}} + b_5\sin^4\phi_{\mathrm{c}},\end{aligned} \tag{30}$$

with the coefficients

$$\begin{aligned}b_1 &= \mathbb{C}_{1111}, \quad b_2 = \mathbb{C}_{1112}+\mathbb{C}_{1121}+\mathbb{C}_{1211}+\mathbb{C}_{2111}, \\ b_3 &= \mathbb{C}_{1122}+\mathbb{C}_{1212}+\mathbb{C}_{1221}+\mathbb{C}_{2112}+\mathbb{C}_{2121}+\mathbb{C}_{2211}, \\ b_4 &= \mathbb{C}_{1222}+\mathbb{C}_{2122}+\mathbb{C}_{2212}+\mathbb{C}_{2221}, \quad b_5 = \mathbb{C}_{2222}.\end{aligned} \tag{31}$$

The second derivatives with respect to ϕ_{c} then take on the forms

$$\frac{\partial^2 q_1}{\partial\phi_{\mathrm{c}}^2} = 2\cos 2\phi_{\mathrm{c}}\left(\sigma_2-\sigma_1\right), \tag{32}$$

$$\frac{\partial^2 q_2}{\partial\phi_{\mathrm{c}}^2} = 2\cos 2\phi_{\mathrm{c}}\left(\lambda_{\mathrm{e},2}^2-\lambda_{\mathrm{e},1}^2\right), \tag{33}$$

$$\begin{aligned}\frac{\partial^2 q_3}{\partial\phi_{\mathrm{c}}^2} &= (-4b_1+2b_3)\cos^4\phi_{\mathrm{c}} + (-10b_2+6b_4)\cos\phi_{\mathrm{c}}\sin^3\phi_{\mathrm{c}} \\ &\quad +(12b_1-12b_3+12b_5)\cos^2\phi_{\mathrm{c}}\sin^2\phi_{\mathrm{c}} \\ &\quad +(6b_2-10b_4)\cos\phi_{\mathrm{c}}\sin^3\phi_{\mathrm{c}} + (2b_3-4b_5)\sin^4\phi_{\mathrm{c}}.\end{aligned} \tag{34}$$

3.4. Initial and boundary conditions

Initially the collagen gel is taken to be stress-free and to have a uniform distribution of collagen fibres $\rho(\phi) = \rho_c(\phi_c) = \rho_0$, i.e. the fibres are uniformly distributed in the $\mathbf{e}_1$-$\mathbf{e}_2$-plane, and reference and current configurations coincide. This stress-free state is associated with the stretches $\lambda_1 = \lambda_2 = \lambda_3 = \lambda_{e,1} = \lambda_{e,2} = \lambda_{e,3} = 1$, and $\lambda_r = 1$. At time $t = 0$, the gel is constrained either biaxially or uniaxially, and the remodelling process starts.

The boundary condition $S_3 = P_3 = \sigma_3 = 0$ holds throughout the analysis. During remodelling of a biaxially constrained gel, the additional kinematic boundary conditions $\lambda_1 = \lambda_2 = 1$ apply. In the case of a uniaxially constrained gel, the boundary conditions $\lambda_1 = 1$ and $S_2 = P_2 = \sigma_2 = 0$ instead apply during remodelling.

After the 72h of remodelling, the gel is exposed to equibiaxial tensile testing in load-control. This implies that the first Piola-Kirchhoff stresses $P_1 = P_2$ are prescribed, and the resulting deformations λ_1 and λ_2 are computed.

3.5. Numerical prerequisites

The remodelling process required a total time of $t_{max} = 72$h to be completed, and time t was discretised using a constant time increment $\Delta t = t_{max}/1000 = 0.072$h. The angular dimension ϕ was discretised using $n_{int} = 50$ integration points. The angles ϕ_i were uniformly distributed in the range $[0, \pi/2]$, according to $\phi_i = \Delta\phi(i - 1/2)$ with $\Delta\phi = \pi/(2n_{int})$. This discretisation proved to be refined enough to yield discretisation-independent results. With regards to the fibre distribution, we introduce the entity ρ', defined as

$$\rho(\phi) = \rho_0 \rho'(\phi). \tag{35}$$

In the computations, the variables $\rho'_1 \dots \rho'_{50}$, associated with the directions $\phi_1 \dots \phi_{50}$, together with the three stretches λ_r, $\lambda_{e,1}$, and $\lambda_{e,2}$, were used as state variables. The remodelling process was analysed by use of an explicit computational scheme. Let index j denote the current, known state, and index $j + 1$ the next state to be computed. As a first step, λ_r is updated by use of Eq. (19). Noting that $J_r = \lambda_r^2$ and that the volume concentration of fibroblasts in the reference configuration ρ_f is related to the current concentration $\rho_{f,c}$ as $\rho_{f,c} = \rho_f/J_r$, the discretised evolution equation becomes

$$\lambda_r^{j+1} = \lambda_r^j - \frac{\alpha \rho_f}{2} \lambda_r^j \Delta t, \tag{36}$$

where $\rho_{\rm f}$ is taken to be constant, implying that the number of fibroblasts is constant during the 72h of remodelling. Updated stretches $\lambda_{\rm e,1}^{j+1}$ and $\lambda_{\rm e,2}^{j+1}$, fulfilling the appropriate kinematic and loading boundary conditions (either $\{\lambda_1 = \lambda_2 = 1\}$ or $\{\lambda_1 = 1,\ S_2 = 0\}$), are then computed. Second Piola-Kirchhoff stresses are computed as

$$\begin{aligned}
\mathbf{S}^j &= 2k_{\rm c}\rho_0 \sum_{i=1}^{n_{\rm int}} (\rho_i')^j \exp\left[a\left(\xi_i^j - 1\right)^2\right]\left(\xi_i^j - 1\right)\mathbf{A}_i \cdot H(\xi_i^j - 1)\Delta\phi \\
&- 2k_{\rm cn}\rho_0 \sum_{i=1}^{n_{\rm int}} (\rho_i')^j \left(\xi_{{\rm c},i} - \xi_i^j\right)\mathbf{A}_i \cdot H(\xi_{{\rm c},i} - \xi_i^j)\Delta\phi \\
&+ k_3\left((\lambda_{e,3}^j)^2 - 1\right)\mathbf{e}_3 \otimes \mathbf{e}_3 - k_3(\lambda_{e,3}^j)^2\left((\lambda_{e,3}^j)^2 - 1\right)\cdot(\mathbf{C}_{\rm e}^j)^{-1},
\end{aligned} \tag{37}$$

where $\xi_i^j = (\lambda_{\rm e,1}^j)^2\cos^2\phi_i + (\lambda_{\rm e,2}^j)^2\sin^2\phi_i$, $\xi_{{\rm c},i} = \lambda_{\rm c,e,1}^2\cos^2\phi_i + \lambda_{\rm c,e,2}^2\sin^2\phi_i$, $\mathbf{A}_i = \cos^2\phi_i \cdot \mathbf{e}_1 \otimes \mathbf{e}_1 + \sin^2\phi_i \cdot \mathbf{e}_2 \otimes \mathbf{e}_2$, $\mathbf{C}_{\rm e}^j = (\lambda_{\rm e,1}^j)^2 \cdot \mathbf{e}_1 \otimes \mathbf{e}_1 + (\lambda_{\rm e,2}^j)^2 \cdot \mathbf{e}_2 \otimes \mathbf{e}_2 + (\lambda_{\rm e,3}^j)^2 \cdot \mathbf{e}_3 \otimes \mathbf{e}_3$, and $\lambda_{e,3}^j = (\lambda_{e,1}^j\lambda_{e,2}^j)^{-1}$. Finally, the state variables ρ_i' are updated by use of Eq's. (13) and (14). The first term in Eq. (13) may be rewritten by use of Eq. (24) according to

$$\frac{\partial\rho_{\rm c}}{\partial t} = \frac{\partial}{\partial t}\left(\frac{\rho}{J_{\rm r}}\frac{\lambda_{\rm e,1}^2 + \lambda_{\rm e,2}^2\tan^2\phi}{\lambda_{\rm e,1}\lambda_{\rm e,2}(1+\tan^2\phi)}\right). \tag{38}$$

This leads to a discretised evolution equation for ρ_i':

$$\begin{aligned}
(\rho_i')^{j+1} &= (\rho_i')^j\left(1 + \frac{\Delta J_{\rm r}^j}{J_{\rm r}^j} + \frac{\Delta\lambda_{\rm e,1}^j}{\lambda_{\rm e,1}^j} + \frac{\Delta\lambda_{\rm e,2}^j}{\lambda_{\rm e,2}^j} - \right. \\
&- \beta\frac{\rho_{\rm f}}{J_{\rm r}^j}\left(\frac{\partial^2 q}{\partial\phi_{\rm c}^2}\right)_i^j\Delta t - \\
&- \left.\frac{2(\lambda_{\rm e,1}^j\Delta\lambda_{\rm e,1}^j + \lambda_{\rm e,2}^j\Delta\lambda_{\rm e,2}^j\tan^2\phi_i)}{(\lambda_{\rm e,1}^j)^2 + (\lambda_{\rm e,2}^j)^2\tan^2\phi_i}\right),
\end{aligned} \tag{39}$$

where $J_{\rm r}^j = (\lambda_{\rm r}^j)^2$, $\Delta J_{\rm r}^j = 2\lambda_{\rm r}^j\Delta\lambda_{\rm r}^j$, $\Delta\lambda_{\rm r}^j = \lambda_{\rm r}^{j+1} - \lambda_{\rm r}^j$, $\Delta\lambda_{\rm e,1}^j = \lambda_{\rm e,1}^{j+1} - \lambda_{\rm e,1}^j$, $\Delta\lambda_{\rm e,2}^j = \lambda_{\rm e,2}^{j+1} - \lambda_{\rm e,2}^j$, $\phi_{{\rm c},i}^j = \arctan(\lambda_{\rm e,2}^j\tan\phi_i/\lambda_{\rm e,1}^j)$, $\sigma_1^j = (\lambda_{\rm e,1}^j)^2 S_1^j$, and $\sigma_2^j = (\lambda_{\rm e,2}^j)^2 S_2^j$. The derivative $(\partial^2 q/\partial\phi_{\rm c}^2)_i^j$ is evaluated by use of the expressions in Eqs. (32)-(34) and (31).

4. Assessment of the three remodelling criteria

The purpose with the present section is to investigate to what extent the three proposed continuum mechanics entities $q_1 = \sigma_{\mathrm{m}}$, $q_2 = \lambda_{\mathrm{m}}^2$, and $q_3 = \mathbb{C}_{\mathrm{m}}$ can be used to predict the activity of fibroblasts as they remodel a collagen gel. However, the constitutive model has a number of parameters that need to be determined first. Thus, we start by exploring the general mechanical behaviour of the proposed constitutive model before we specifically address the issue of fibre reorientation.

In the present problem formulation, the model behaviour is governed by the parameters $k_{\mathrm{c}}\rho_0$, a, $k_{\mathrm{cn}}\rho_0$, k_3, $\alpha\rho_{\mathrm{f}}$, and $\beta\rho_{\mathrm{f}}$, where the influence of $\beta\rho_{\mathrm{f}}$ is the most interesting, since the evolution law Eq. (13) for fibre reorientation depends directly on this parameter. Thomopoulos et al. (2007) present experimental results in terms of remodelled collagen fibre distributions, stress-strain relations, and remodelling strains. We start by considering a case with $q = q_1 = \sigma_{\mathrm{m}}$. In this case, the parameter set $k_{\mathrm{c}}\rho_0 = 150\mathrm{Pa}$, $a = 20$, $k_{\mathrm{cn}}\rho_0 = 600\mathrm{Pa}$, $k_3 = 75\mathrm{Pa}$, $\alpha\rho_{\mathrm{f}} = 0.003\mathrm{s}^{-1}$, and $\beta\rho_{\mathrm{f}} = 0.00043\mathrm{Pa}^{-1}\mathrm{s}^{-1}$ provided the best fit to the experimental data.

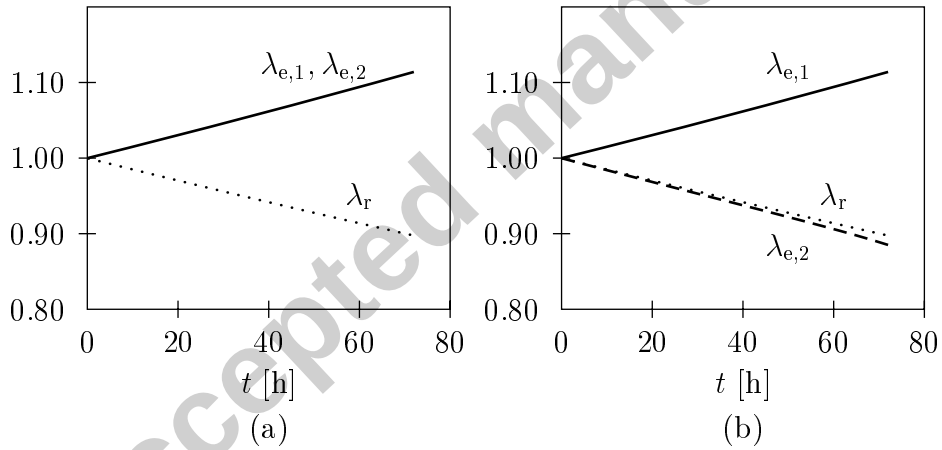

Figure 4: Evolution of state variables $\lambda_{\mathrm{e},1}$, $\lambda_{\mathrm{e},2}$, and λ_{r} during the 72h of remodelling: (a) biaxially constrained gel; (b) uniaxially constrained gel. Solid, dashed, and dotted lines pertain to $\lambda_{\mathrm{e},1}$, $\lambda_{\mathrm{e},2}$, and λ_{r}, respectively. Remodelling criterion: $q = q_1$. Model parameters: $k_{\mathrm{c}}\rho_0 = 150\mathrm{Pa}$, $a = 20$, $k_{\mathrm{cn}}\rho_0 = 600\mathrm{Pa}$, $k_3 = 75\mathrm{Pa}$, $\alpha\rho_{\mathrm{f}} = 0.003\mathrm{s}^{-1}$, and $\beta\rho_{\mathrm{f}} = 0.00043\mathrm{Pa}^{-1}\mathrm{s}^{-1}$.

Fig. 4 shows the predicted evolution of the state variables $\lambda_{\mathrm{e},1}$, $\lambda_{\mathrm{e},2}$, and λ_{r}

during the remodelling process for this set of model parameters. Figs. 4(a) and (b) pertain to biaxially and uniaxially constrained gels, respectively. In the biaxially constrained gel in Fig. 4(a), $\lambda_{e,1}$ and $\lambda_{e,2}$ are equal, due to symmetry. Since λ_r starts at 1 and then decreases, $\lambda_{e,1}$ and $\lambda_{e,2}$ start at 1 and increase to fulfil the kinematic constraints $\lambda_1 = \lambda_2 = 1$. Due to incompressibility, $\lambda_{e,3} = (\lambda_{e,1}\lambda_{e,2})^{-1}$ is less than 1 in the biaxially constrained gel.

In the uniaxially constrained gel in Fig. 4(b), the predicted evolution paths of $\lambda_{e,1}$ and λ_r are identical to the corresponding curves for the biaxially constrained gel, whereas $\lambda_{e,2}$ is now instead located just below λ_r. In this case, the $\mathbf{e}_2$-direction is unconstrained. Due to the boundary condition $S_2 = 0$ and incompressibility, the elastic stretch $\lambda_{e,2}$ is below 1 and collagen fibres oriented in the $\mathbf{e}_2$-direction are therefore in a state of compression. In the uniaxially constrained gel, $\lambda_{e,3}$ is predicted to be slightly above 1.

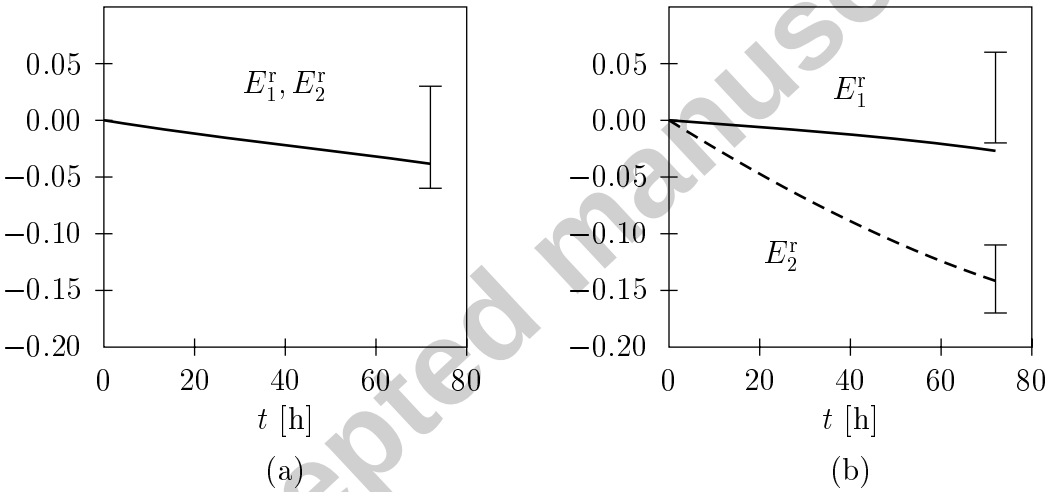

Figure 5: Predicted remodelling strains for gels during the 72h of remodelling: (a) biaxially constrained gel; (b) uniaxially constrained gel. Solid and dashed lines denote model predictions of E_1^r and E_2^r, respectively. Remodelling criterion: $q = q_1$. Model parameters: $k_c\rho_0 = 150$Pa, $a = 20$, $k_{cn}\rho_0 = 600$Pa, $k_3 = 75$Pa, $\alpha\rho_f = 0.003\text{s}^{-1}$, and $\beta\rho_f = 0.00043\text{Pa}^{-1}\text{s}^{-1}$.

After the 72h of remodelling, the constraints were removed from the collagen gels. The gels would then go to their load-free configurations. Thomopoulos et al. present remodelling strains E_1^r and E_2^r, which are Green

strains defined as the deformation from the undeformed, initial state before remodelling to the load-free state after remodelling. For the biaxially constrained gels, the remodelling strains $E_1^{\mathrm{r}} = -0.01 \pm 0.04$ and $E_2^{\mathrm{r}} = -0.03 \pm 0.03$ were obtained by Thomopoulos et al. For the uniaxially constrained gels, the corresponding values were $E_1^{\mathrm{r}} = 0.02 \pm 0.04$ and $E_2^{\mathrm{r}} = -0.14 \pm 0.03$. (Values are given in terms of averages and standard deviations for the 36 gels used by Thomopoulos et al.) The predicted evolution of the remodelling strains E_1^{r} and E_2^{r} for the biaxially and uniaxially constrained gels are displayed in Fig. 5(a) and (b), respectively. The confidence intervals for the experimental E_1^{r} and E_2^{r} values are indicated at $t = 72$h. The magnitude of the predicted remodelling strains increases monotonically with time in both the biaxially and uniaxially constrained gels. For the biaxially constrained gel in Fig. 5(a), the predicted final remodelling strain are within the confidence limits obtained from the experimental results.

For the uniaxially constrained gel in Fig. 5(b), there is a significant difference between the 1- and 2-directions. Since the $\mathbf{e}_2$-direction is unconstrained during remodelling, the gel is free to contract in this direction. At the end of the analysis, the experimental average $E_2^{\mathrm{r}} = -0.14$ is accurately predicted. The prediction of E_1^{r} is not as accurate, and the model slightly overestimates the magnitude of the remodelling strain in the $\mathbf{e}_1$-direction.

Thomopoulos et al. also present stress-strain relations for the remodelled collagen gels, and these data are reproduced in Fig. 6. Enclosed are also the associated model predictions. These relations are given in terms of the Green strain vs. second Piola-Kirchhoff stress, obtained from tests with prescribed first Piola-Kirchhoff stresses $P_1 = P_2$. Starting with the biaxially constrained gel in Fig. 6(a), we first note that due to symmetry, the predicted stress-strain curves are the same for the two principal directions. Ideally, the experimental response would also be the same in the 1 and 2 directions, but some deviations can be observed in Fig. 6(a).

Results for the uniaxially constrained gel are shown in Fig. 6(b). There is a significant discrepancy in stiffness between the two principal directions. This is a combined effect of the non-uniform fibre distribution (displayed below) and the pre-stretching of collagen fibres. The pre-stretching of fibres is the key mechanism in the model that explains the large discrepancies in stiffness, on the one hand, between the biaxially and uniaxially constrained gels, and on the other hand, between the two principal directions in the uniaxially constrained gel.

The data from the study of Thomopoulos et al. that are of primary inter-

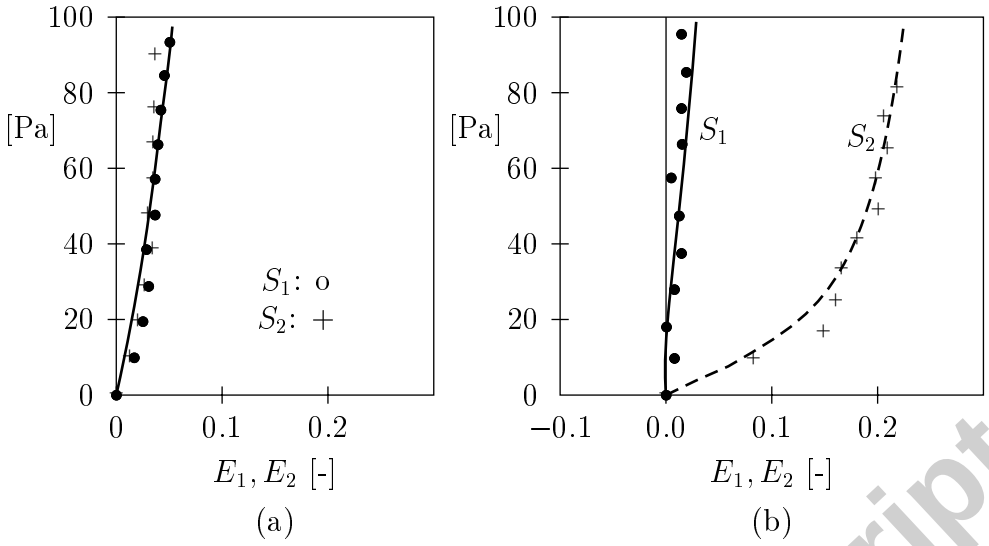

Figure 6: Predicted stress-strain relations for equibiaxial tension tests on gels after 72h of remodelling: (a) biaxially constrained gel; (b) uniaxially constrained gel. Symbols denote experimental measurements from Thomopoulos et al. (2007), and solid and dashed lines denote model predictions. Model predictions of S_1 and S_2 are indicated by solid and dashed lines, respectively. Remodelling criterion: $q = q_1$. Model parameters: $k_c\rho_0 = 150$Pa, $a = 20$, $k_{cn}\rho_0 = 600$Pa, $k_3 = 75$Pa, $\alpha\rho_f = 0.003\text{s}^{-1}$, and $\beta\rho_f = 0.00043\text{Pa}^{-1}\text{s}^{-1}$.

est in the present investigation are the histological data for the remodelled collagen gels in terms of distributions of fibre orientations. Fibre distributions are displayed in terms of the normalised entity $\bar{\rho}_c$, defined as

$$\bar{\rho}_c(\phi_c) = \frac{\rho_c(\phi_c)}{\int_{\phi_c=-\pi/2}^{\pi/2} \rho_c(\phi_c)\mathrm{d}\phi_c} = \frac{\rho'_c(\phi_c)}{\int_{\phi_c=-\pi/2}^{\pi/2} \rho'_c(\phi_c)\mathrm{d}\phi_c}, \tag{40}$$

where ρ'_c relates to ρ' according to Eq. (24). (Note that $\bar{\rho}_c(\phi_c)$ is a density function in a statistical sense, which $\rho_c(\phi_c)$, $\rho'_c(\phi_c)$, $\rho(\phi)$, and $\rho'(\phi)$, in general, are not.)

Fig. 7 shows the experimentally obtained collagen fibre distribution after 72h of remodelling in a biaxially constrained gel. The distribution pertain to the load-free state of the gel after remodelling. Enclosed in Fig. 7 are also the fibre distributions predicted by the model for $q = q_1$. Model predictions are shown for four different values of the fibre reorientation rate $\beta\rho_f$: 0, $0.0002\text{Pa}^{-1}\text{s}^{-1}$, $0.00043\text{Pa}^{-1}\text{s}^{-1}$, and $0.0008\text{Pa}^{-1}\text{s}^{-1}$. The experimental data

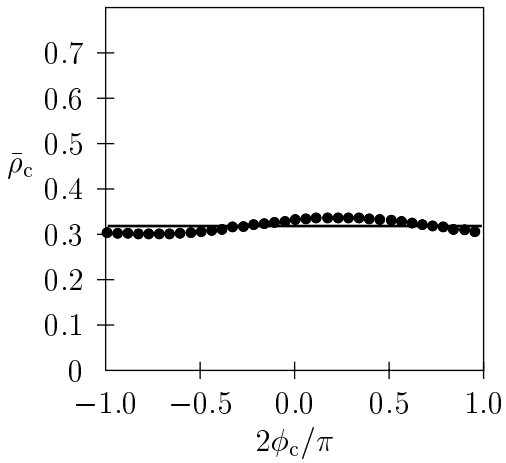

Figure 7: Predicted fibre distribution in biaxially constrained gel after 72h of remodelling for $q = q_1 = \sigma_m$. Symbols denote experimental measurements from Thomopoulos et al. (2007) and solid lines denote model predictions for $\beta\rho_f = 0$, $2{\cdot}10^{-4}\text{Pa}^{-1}\text{s}^{-1}$, $4.3{\cdot}10^{-4}\text{Pa}^{-1}\text{s}^{-1}$, and $8{\cdot}10^{-4}\text{Pa}^{-1}\text{s}^{-1}$. Other model parameters: $k_c\rho_0 = 150\text{Pa}$, $a = 20$, $k_{cn}\rho_0 = 600\text{Pa}$, $k_3 = 75\text{Pa}$, and $\alpha\rho_f = 0.003\text{s}^{-1}$.

shows some variation, but essentially makes up a uniform distribution. The distribution predicted by the model is perfectly uniform, and predictions for different values of $\beta\rho_f$ collapse to a single line. Even in the biaxially constrained case, the gel is actually remodelled, but the remodelling occurs isotropically in terms of λ_r and no redistribution of the fibre density $\bar{\rho}_c$ occurs. Thus, the normalised entity $\bar{\rho}_c(\phi_c)$ remains uniform. Note that the non-normalised entity $\rho_c(\phi_c)$ also remains uniform (not shown), but the amplitude of it will evolve with time at a rate that depends on the contraction rate $\alpha\rho_f$. Due to symmetry, the predicted fibre distribution in the biaxially constrained gel will always remain uniform independently of parameter variations, and it will therefore not be displayed in the following. Instead we focus on the fibre distribution in the uniaxially constrained gel.

Figs. 8(a) and (b) show the predicted stress and fibre distributions after remodelling for the uniaxially constrained gel. In Fig. 8(b), the experimental fibre distribution is also enclosed. The stress profiles in (a) pertain to the *constrained* gel at $t = 72\text{h}$, whereas the fibre distributions in (b) pertain to the *unconstrained*, load-free gel. The amplitude of the predicted end-profiles of the stress in Fig. 8(a) increases with increasing reorientation rate $\beta\rho_f$.

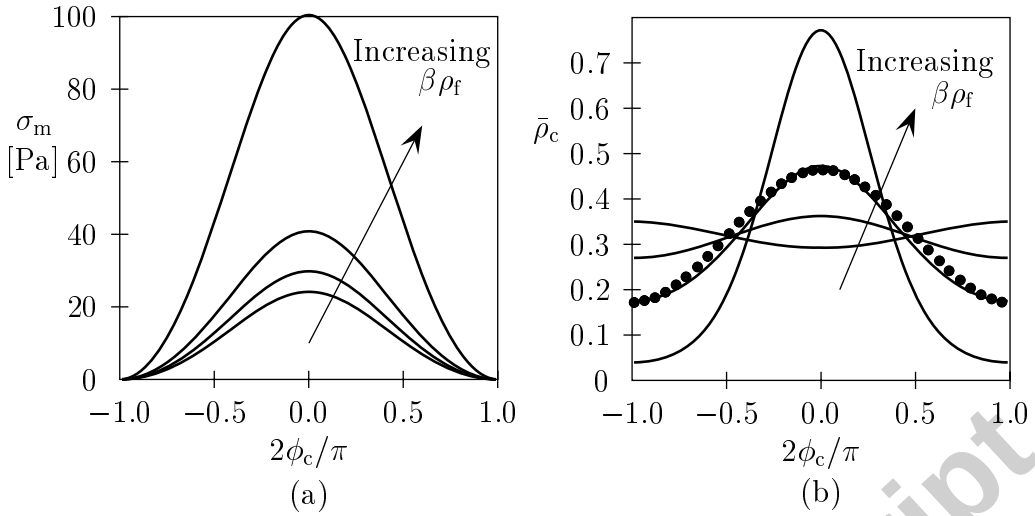

Figure 8: Predicted stress and fibre orientation distributions in a uniaxially constrained gel after 72h of remodelling for $q = q_1 = \sigma_m$: (a) predicted stress distributions; (b) predicted fibre orientation distributions. Symbols denote experimental measurements from Thomopoulos et al. (2007) and solid lines denote model predictions for $\beta\rho_f = 0$, $2{\cdot}10^{-4}\text{Pa}^{-1}\text{s}^{-1}$, $4.3{\cdot}10^{-4}\text{Pa}^{-1}\text{s}^{-1}$, and $8{\cdot}10^{-4}\text{Pa}^{-1}\text{s}^{-1}$. Other model parameters: $k_c\rho_0 = 150\text{Pa}$, $a = 20$, $k_{cn}\rho_0 = 600\text{Pa}$, $k_3 = 75\text{Pa}$, and $\alpha\rho_f = 0.003\text{s}^{-1}$.

The reason is that the higher value of $\beta\rho_f$, the more fibres are aligned in the $\mathbf{e}_1$-direction at the end of the analysis. For a given value of λ_r and $\lambda_{e,1}$, this will result in an increasing stress in the $\mathbf{e}_1$-direction.

Turning to the fibre distribution profiles in Fig. 8(b), we note that the predicted distribution for $\beta\rho_f = 0$ is not uniform (as might be expected). In fact, after the remodelling there are slightly more fibres (predicted to be) oriented in the $\mathbf{e}_2$-direction than in the $\mathbf{e}_1$-direction. The fibre distribution in the constrained state during remodelling does indeed remain uniform. But as the constraint is removed, the gel undergoes an elastic deformation as it shrinks back to its load-free state, and it is the fibre distribution in this load-free state that is shown in Fig. 8(b). Thus, the non-uniformity observed in the predicted fibre distribution for $\beta\rho_f = 0$ is produced by this elastic recoil.

For increasing values of reorientation rate $\beta\rho_f$, the fibres tend to align more and more in the constrained $\mathbf{e}_1$-direction, and the resulting fibre distribution becomes increasingly non-uniform, as seen in Fig. 8(b). A value $\beta\rho_f = 0.00043\text{Pa}^{-1}\text{s}^{-1}$ enables a very good prediction of the experimental fi-

bre distribution. The predicted stress-strain relations of the remodelled gels also depend on $\beta\rho_{\mathrm{f}}$, but these are not displayed.

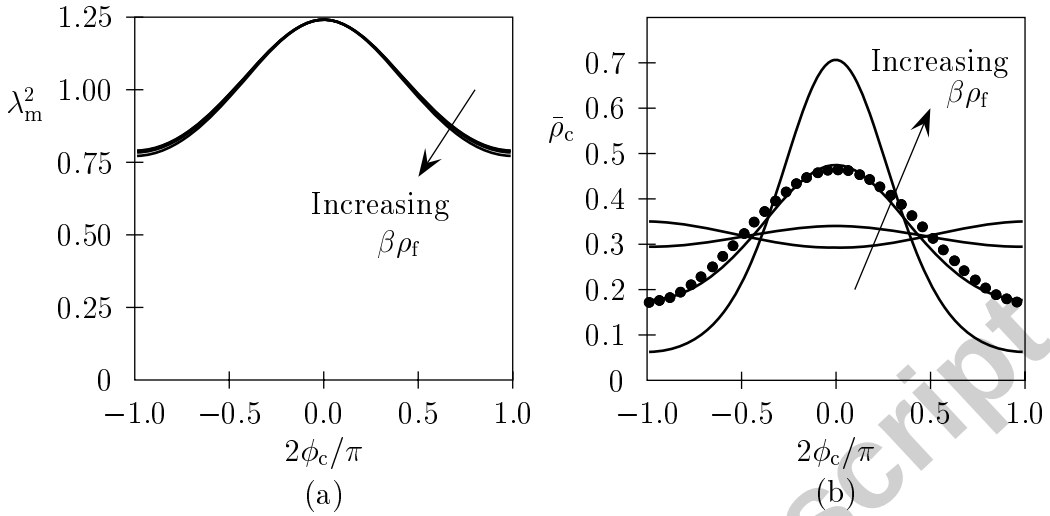

Figure 9: Predicted elastic deformation and fibre orientation distributions in a uniaxially constrained gel after 72h of remodelling for $q = q_2 = \lambda_{\mathrm{m}}^2$: (a) predicted distributions of elastic deformation; (b) predicted fibre orientation distributions. Symbols denote experimental measurements from Thomopoulos et al. (2007) and solid lines denote model predictions for $\beta\rho_{\mathrm{f}} = 0$, $0.005\mathrm{s}^{-1}$, $0.018\mathrm{s}^{-1}$, and $0.04\mathrm{s}^{-1}$. Other model parameters: $k_{\mathrm{c}}\rho_0 = 150\mathrm{Pa}$, $a = 20$, $k_{\mathrm{cn}}\rho_0 = 600\mathrm{Pa}$, $k_3 = 75\mathrm{Pa}$, and $\alpha\rho_{\mathrm{f}} = 0.003\mathrm{s}^{-1}$.

The second remodelling criterion $q = q_2 = \lambda_{\mathrm{m}}^2$ is now considered. Figs. 9(a) and (b) show the predicted end-distributions of the elastic deformation λ_{m}^2 and the fibre orientation, respectively, for the reorientation rates $\beta\rho_{\mathrm{f}} = 0$, $0.05\mathrm{s}^{-1}$, $0.18\mathrm{s}^{-1}$, and $0.40\mathrm{s}^{-1}$. (Note that the unit of β changes with the unit of q.) The profiles of the elastic deformation for the different values of $\beta\rho_{\mathrm{f}}$ in (a) do not vary much. The remodelling stretch λ_{r} is essentially prescribed, and the elastic stretch $\lambda_{\mathrm{e},1}$ is then also defined due to the boundary condition $\lambda_1 = 1$. Furthermore, due to the relatively high value of k_{cn}, the elastic stretch $\lambda_{\mathrm{e},2}$ does not change much either with $\beta\rho_{\mathrm{f}}$.

The general shape of the predicted fibre distributions in (b), obtained for $q = q_2$, clearly resemble the profiles obtained for $q = q_1$ in Fig. 8(b). There is also the same tendency that the higher the value of the reorientation rate $\beta\rho_{\mathrm{f}}$, the more fibres end up being aligned in the constrained $\mathbf{e}_1$-direction. The best agreement with experiments is attained for $\beta\rho_{\mathrm{f}} = 0.18\mathrm{s}^{-1}$, and this

prediction is virtually just as good as for $q = q_1$. For this value of $\beta\rho_\mathrm{f}$, the experimental stress-strain data in Fig. 6 are also accurately predicted (not shown).

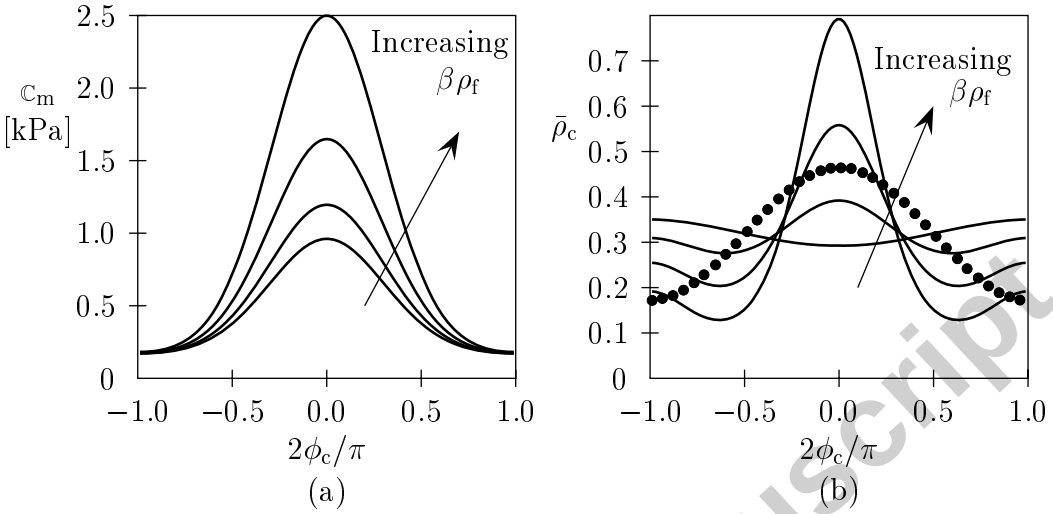

Figure 10: Predicted stiffness and fibre orientation distributions in a uniaxially constrained gel after 72h of remodelling for $q = q_3 = \mathbb{C}_\mathrm{m}$: (a) predicted stiffness distributions; (b) predicted fibre orientation distributions. Symbols denote experimental measurements from Thomopoulos et al. (2007) and solid lines denote model predictions for $\beta\rho_\mathrm{f} = 0$, $5{\cdot}10^{-6}\mathrm{Pa}^{-1}\mathrm{s}^{-1}$, $1{\cdot}10^{-5}\mathrm{Pa}^{-1}\mathrm{s}^{-1}$, and $1.4{\cdot}10^{-5}\mathrm{Pa}^{-1}\mathrm{s}^{-1}$. Other model parameters: $k_\mathrm{c}\rho_0 = 150\mathrm{Pa}$, $a = 20$, $k_\mathrm{cn}\rho_0 = 600\mathrm{Pa}$, $k_3 = 75\mathrm{Pa}$, and $\alpha\rho_\mathrm{f} = 0.003\mathrm{s}^{-1}$.

As a last step in this assessment, we now investigate the third remodelling criterion, $q = q_3 = \mathbb{C}_\mathrm{m}$. In Figs. 10(a) and (b), the predicted stiffness and fibre distributions for $q = q_3$ are provided. Predictions are shown for reorientation rates $\beta\rho_\mathrm{f} = 0$, $5{\cdot}10^{-6}\mathrm{Pa}^{-1}\mathrm{s}^{-1}$, $1{\cdot}10^{-5}\mathrm{Pa}^{-1}\mathrm{s}^{-1}$, and $1.4{\cdot}10^{-5}\mathrm{Pa}^{-1}\mathrm{s}^{-1}$.

In the stiffness profiles in Fig. 10(a), pertaining to the constrained gel at the end of the analysis, the predicted stiffness in the $\mathbf{e}_1$-direction increases with increasing $\beta\rho_\mathrm{f}$. This is a result of the fact that for increasing $\beta\rho_\mathrm{f}$, more fibres are aligned in the $\mathbf{e}_1$-direction at the end of the analysis. It may be noted, that the predicted stiffness in the $\mathbf{e}_2$-direction essentially is independent of $\beta\rho_\mathrm{f}$ and of variations in fibre density (see Fig. 10(b)). The explanation is that fibres oriented in the $\mathbf{e}_2$-direction are in a state of compression. This holds both for the constrained gel and for the load-free gel when the constraint is removed. The stiffness in the $\mathbf{e}_2$-direction is not governed by the

fibre density but rather by the stiffness parameter k_3, see Eq. (27). The hydrostatic stress component in the gel is governed by k_3, and the hydrostatic stress also contributes to the stiffness tensor, as seen in Eq. (27). Hence, in the $\mathbf{e}_1$-direction, the material stiffness is dominated by the fibre contribution, but close to the $\mathbf{e}_2$-direction, the fibre contribution vanishes, and the stiffness approaches a value determined by k_3.

In Fig. 10(b), the predicted fibre distributions are displayed. It is clear, that the remodelling criterion $q_3 = \mathbb{C}_{\mathrm{m}}$ is not able to reproduce the experimental fibre distribution. The basic problem is that criterion q_3 does not predict a fibre density that decreases monotonically from the $\mathbf{e}_1$-direction to the $\mathbf{e}_2$-direction. Instead, a minimum in fibre density is predicted to appear at $\phi_{\mathrm{c}} \approx \pm 0.3\pi$.

Since the stiffness close to the $\mathbf{e}_2$-direction is governed by k_3, lower values of k_3 were also tried, to see if this could improve the predicted profiles for the fibre distribution, but to no avail. The only outcome was that the associated predictions of the stress-strain profiles became significantly worse.

5. Discussion and concluding remarks

Collagen fabrics and networks play a very important mechanical role in the human body, and the ability of collagen fibre networks to grow and remodel themselves enables them to adjust to varying physiological conditions. The maintenance of these fibre networks is performed by fibre-producing cells, such as fibroblasts. The evolution of these fibre networks is strongly dependent upon the interaction between the cells and the surrounding extracellular matrix. The activity of the cells is of pivotal importance for the mechanical behaviour of collagenous tissues, and therefore needs to be included in a material description of this material. Continuum mechanics is a very powerful tool when modelling deformable solids, and if continuum mechanics measures, such as stress, strain or stiffness, can be correlated with cell activity, much is to be gained from the modelling point of view.

In the present paper, we investigate to what extent continuum mechanics entities can be correlated with or used to predict the activity of fibroblasts in terms of their reorientation of collagen fibres during collagen gel remodelling. For this purpose, a continuum mechanics framework and a constitutive model for the collagen fabric were adopted. The continuum mechanics treatment is similar to the one proposed by Rodriguez et al. (1994), where the total deformation gradient is decomposed into an inelastic part, associated with

growth and remodelling, and an elastic part, required to fulfil equilibrium. Fibroblasts are assumed to accomplish a pre-stretching of collagen fibres, and due to cross-linking and interactions between fibres, fibres do not attain their load-free state upon removal of external loads or constraints, but remain partly stretched. The orientation of collagen fibres in space is described by a density function, defined over the unit sphere. Fibroblasts are assumed to reorient fibres towards the direction of either increasing Cauchy stress, elastic deformation, or current stiffness. This reorientation process is modelled by use of a diffusion-like evolution law for the collagen density.

In the present model, the remodelling of the collagen fabric accomplished by the fibroblasts is taken to consist of two parts: an isotropic contraction that is independent of the external loads and a pure reorientation of fibres that depends on the stress or deformation state. Physically, this assumption means that under the present experimental conditions, the stresses and deformations caused by the external constraints are assumed to be relatively low compared with the contraction strength of the fibroblasts, i.e fibroblast contraction is not affected by the external constraints. On the other hand, the influence of the external constraints is strong enough to tell the cells how the collagen should be reoriented.

When studying remodelling of collagen networks, collagen gels are often employed (see e.g. Pedersen and Swartz (2005) for a review). The advantage of these gels is that the features of collagen can be studied more or less in isolation compared to the situation in real tissues. These gels are often based on type I collagen, which may be purified from rat tail tendon or bovine cartilage by acid digestion. To these gels, fibroblasts are typically added to study remodelling of the collagen network. Remodelling of both uniaxially and biaxially constrained collagen gels has been investigated, e.g. in Balestrini and Billiar (2009); Huang et al. (1993); Kessler et al. (2001); Thomopoulos et al. (2005, 2007), where the resulting changes in structural organisation and mechanical properties of the gel are examined. In the present study, experimental results presented by Thomopoulos et al. (2007) were used. Thomopoulos et al. investigated the histological and mechanical properties of collagen gels that had undergone remodelling under both biaxial and uniaxial constraint. More specifically, Thomopoulos et al. investigated the distribution of collagen fibre orientation after the remodelling process, and they also performed biaxial mechanical tensile testing of the gels.

As the three remodelling criteria were applied, the numerical results indicated, that criteria 1 and 2 (Cauchy stress and elastic deformations) were

suitable for predicting the evolution of the collagen fibre distribution. Criteria 1 and 2 yielded essentially equally good predictions of the collagen fibre distribution after 72h of remodelling of a uniaxially constrained gel. When applying criterion 3 (current stiffness), the model was not able to reproduce the experimental distribution. Since the stiffness in the $\mathbf{e}_2$-direction is, in fact, not governed by the fibre density but by k_3, it could be conjectured, that it is the choice of k_3 that is the problem and not the remodelling criterion as such. However, other values of k_3 were explored, and also other combinations of the remaining model parameters, but a proper prediction of the fibre density for criterion 3 could not be attained. Thus, the present analysis indicates that the Cauchy stress and the elastic deformation in the collagen gel can be used to predict collagen remodelling, whereas the current stiffness of the gel is not suitable for this purpose. However, this conclusion is tentative and depends on the overall physical soundness of the theoretical framework employed. Furthermore, the conclusion cannot necessarily be generalised to cell activities in general. Fibroblasts and other cells have a spectrum of activities, and in the present analysis, only one activity (i.e. fibre remodelling) was considered.

Several theoretical studies have focused on the mechanical behaviour of collagen gels and collagen networks, e.g. Barocas and Tranquillo (1997); Chandran and Barocas (2006); Driessen et al. (2003); Farquhar et al. (1990); Kroon (2009); Lanir (1979a); Ohsumi et al. (2008); Soulhat et al. (1999), and some of these (Barocas and Tranquillo, 1997; Driessen et al., 2003; Kroon, 2009; Ohsumi et al., 2008) have considered remodelling. In Driessen et al. (2003) the fibre distribution is represented by a structural tensor that evolves with time, and the evolution of the fibre distribution depends on the present deformations in the material. In Kroon (2009), the collagen network is represented by a discrete set of collagen fibres, whose directions may change over time. In that study, the evolution of the fibre directions is taken to depend on the current stiffness of the material. In Barocas and Tranquillo (1997) and Ohsumi et al. (2008), reorientation of collagen fibres is a consequence of anisotropic compaction of the collagen fabric.

Other theoretical studies focus on the remodelling of mature collagen networks. For example, a number of works related to vascular mechanics have been published, e.g. Baek et al. (2006); Humphrey and Rajagopal (2002); Kroon and Holzapfel (2007, 2008, 2009); Eriksson et al. (2009); Watton et al. (2004)). In these studies, the turnover of collagen - i.e. the continuously ongoing process of degradation and production of fibres - is taken to be the

driving mechanism in collagen fibre remodelling. Some studies (e.g. Baek et al. (2006); Driessen et al. (2004)) also include effects of local collagen fibre reorientation. Baek et al. (2006) investigate reorientation of fibres using different criteria for the preferred direction, such as direction of maximum principal stress and maximum principal stretch. Baek et al. studied growth of fusiform aneurysms, and in that context, the use of principal stretches appeared to be the most appropriate. Driessen et al. (2004) also use the maximum principal stretch to define the preferred direction towards which the collagen fibres strive during the remodelling process.

The correlation between continuum mechanics entities and cell activity needs to be further investigated. The theoretical framework proposed here could be applied to experiments where more advanced boundary conditions are imposed. The direction of constraint or applied load could, for example, be changed during the course of the experiment. If possible, biaxial mechanical testing of the gel and histological examinations of the collagen structure could also be performed at several stages of remodelling in such a test, and not just at the end of it. Such an approach would allow for a more complete assessment of the proposed framework.

In summary, a theoretical framework for the study of remodelling collagen gels has been employed to assess three different criteria for collagen fibre reorientation. The constitutive model for the collagen fabric is formulated in terms of a strain energy function, which includes a density function describing the distribution of the collagen fibre orientation. This density function evolves according to an evolution law, where fibres tend to reorient towards either the direction of increasing Cauchy stress, elastic deformation, or stiffness. The theoretical framework was applied to experimental results from collagen gels, where gels had undergone remodelling under both biaxial and uniaxial constraint. The analyses indicated that criteria 1 and 2 are able to predict the collagen fibre distribution after remodelling, whereas criterion 3 is not. This conclusion is, however, tentative and pertains, strictly speaking, only to remodelling processes, and may not be valid for other types of cell activities.

References

Albrecht-Buehler, G., 1987. Role of cortical tension in fibroblast shape and movement. Cell Motil. Cytoskeleton 7, 54–67.

Annovazzi, L., Genna, F., 2009. An engineering, multiscale constitutive model for fiber-forming collagen in tension. J. Biomed. Mater. Res. AIn press.

Baek, S., Rajagopal, K. R., Humphrey, J. D., 2006. A theoretical model of enlarging intracranial fusiform aneurysms. J. Biomech. Eng. 128, 142–149.

Balestrini, J. L., Billiar, K. L., 2009. Magnitude and duration of stretch modulate fibroblast remodeling. J. Biomech. Eng.In press.

Bao, G., Suresh, S., 2003. Cell and molecular mechanics of biological materials. Nat. Mater. 2, 715–725.

Barocas, V. H., Tranquillo, R. T., 1997. An anisotropic biphasic theory of tissue-equivalent mechanics: The interplay among cell traction, fibril alignment, and cell contact guidance. J. Biomech. Eng. 119, 137–145.

Birk, D. E., Zycband, E. I., Winkelmann, D. A., Trelstad, R. L., 1990. Collagen fibrillogenesis in situ. Discontinuous segmental assembly in extracellular compartments. Ann. N.Y. Acad. Sci. 580, 176–194.

Bishop, J. E., Lindahl, G., 1999. Regulation of cardiovascular collagen synthesis by mechanical load. Cardiovasc. Res. 42, 27–44.

Buckley, C. P., Lloyd, D. W., Konopasek, M., 1980. On the deformation of slender filaments with planar crimp: theory, numerical solution and applications to tendon collagen and textile materials. Proc. R. Soc. Lond. A A 372, 33–64.

Chandran, P. L., Barocas, V. H., 2006. Affine versus non-affine fibril kinematics in collagen networks: theoretical studies of network behavior. J. Biomech. Eng. 128, 259–270.

Cisneros, D. A., Hung, C., Franz, C. M., Muller, D. J., 2006. Observing growth steps of collagen self-assembly by time-lapse high-resolution atomic force microscopy. J. Struct. Biol. 154, 232–245.

Comninou, M., Yannas, I. V., 1976. Dependence of stress-strain nonlinearity of connective tissues on the geometry of collagen fibers. J. Biomech. 9, 427–433.

Cukierman, E., Pankov, R., Stevens, D. R., Yamada, K. M., 2001. Taking cell–matrix adhesions to the third dimension. Science 294, 1708–1712.

Diamant, J., Keller, A., Baer, E., Litt, M., Arridge, R. G. C., 1972. Collagen: Ultrastructure and its relation to mechanical properties as a function of ageing. Proc. R. Soc. Lond. B 180, 293–315.

Driessen, N. J. B., Peters, G. W. M., Huyghe, J. M., Bouten, C. V. C., Baaijens, F. P. T., 2003. Remodelling of continuously distributed collagen fibres in soft connective tissue. J. Biomech. 36, 1151–1158.

Driessen, N. J. B., Wilson, W., Bouten, C. V. C., Baaijens, F. P. T., 2004. A computational model for collagen fibre remodelling in the arterial wall. J. Theor. Biol. 226, 53–64.

Engler, A., Bacakova, L., Newman, C., Hategan, A., Griffin, M., Discher, D., 2004. Substrate compliance versus ligand density in cell on gel responses. Biophys. J. 86, 617–628.

Eriksson, T., Kroon, M., Holzapfel, G. A., 2009. Influence of medial collagen organization and axial in situ stretch on saccular cerebral aneurysm growth. J. Biomech. Eng.In press.

Evans, E., Yeung, A., 1989. Apparent viscosity and cortical tension of blood granulocytes determined by micropipet aspiration. Biophys. J. 56, 151–160.

Farquhar, T., Dawson, P. R., Torzilli, P. A., 1990. A microstructural model for the anisotropic drained stiffness of articular cartilage. J. Biomech. Eng. 112, 414–425.

Friedl, P., Bröcker, E.-B., 2000. The biology of cell locomotion within three-dimensional extracellular matrix. Cell. Mol. Life Sci. 57, 42–64.

Friedrichs, J., Taubenberger, A., Franz, C. M., Muller, D. J., 2007. Cellular remodeling of individual collagen fibrils visualized by time–lapse AFM. J. Mol. Biol. 372, 594–607.

Fung, Y. C., 1967. Elasticity of soft tissues in simple elongation. Am. J. Physiol. 213, 1532–1544.

Gardel, M. L., Valentine, M. T., Crocker, J. C., Bausch, A. R., Weitz, D. A., 2003. Microrheology of entangled f-actin solutions. Phys. Rev. Lett. 91, 1–4.

Grinnell, F., 2003. Fibroblast biology in three–dimensional collagen matrices. Trends in Cell Biology 13, 264–269.

Heidemann, S. R., Kaech, S., Buxbaum, R. E., Matus, A., 1999. Direct observations of the mechanical behaviors of the cytoskeleton in living fibroblasts. J. Cell Biol. 145, 109–122.

Hinz, B., Gabbiani, G., 2003. Mechanisms of force generation and transmission by myofibroblasts. Current Opinion in Biotechnology 14, 538–546.

Huang, D., Chang, T. R., Aggarwal, A., Lee, R. C., Ehrlich, H. P., 1993. Mechanisms and dynamics of mechanical strengthening in ligament-equivalent fibroblast-populated collagen matrices. Ann. Biomed. Eng. 21, 289–305.

Humphrey, J. D., 2001. Stress, strain and mechanotransduction in cells. J. Biomech. Eng. 123, 638–641.

Humphrey, J. D., Rajagopal, K. R., 2002. A constrained mixture model for growth and remodeling of soft tissues. Math. Model. Meth. Appl. Sci. 12, 407–430.

Hurschler, C., Loitz-Ramage, B., Vanderby Jr., R., 1997. A structurally based stress-stretch relationship for tendon and ligament. J. Biomech. Eng. 119, 392–399.

Jiang, H., Grinnell, F., 2005. Cell–matrix entanglement and mechanical anchorage of fibroblasts in three–dimensional collagen matrices. Molecular Biol. Cell 16, 5070–5076.

Kessler, D., Dethlefsen, S., Haase, I., Plomann, M., Hirche, F., Krieg, R., Eckes, B., 2001. Fibroblasts in mechanically stressed collagen lattices assume a 'synthetic' phenotype. J. Bio. Chem. 276, 36575–36585.

Kroon, M., 2009. Modelling of fibroblast-controlled strengthening and remodelling of uniaxially constrained collagen gels. J. Biomech. Eng.In press.

Kroon, M., Holzapfel, G. A., 2007. A model for saccular cerebral aneurysm growth by collagen fibre remodelling. J. Theor. Biol. 247, 775–787.

Kroon, M., Holzapfel, G. A., 2008. Modelling of saccular aneurysm growth in a human middle cerebral artery. J. Biomech. Eng. 130, 1–10.

Kroon, M., Holzapfel, G. A., 2009. A theoretical model for fibroblast-controlled growth of saccular cerebral aneurysms. J. Theor. Biol. 257, 73–83.

Lanir, Y., 1978. Structure-function relations in mammalian tendon: the effect of geometrical nonuniformity. Bioeng. 2, 119–128.

Lanir, Y., 1979a. Rheological behavior of skin–experimental results and a structural model. Biorheology 16, 191–202.

Lanir, Y., 1979b. A structural theory for the homogeneous biaxial stress-strain relationships in flat collagenous tissues. J. Biomech. 12, 423–436.

Lin, H., Clegg, D. O., Lal, R., 1999. Imaging real–time proteolysis of single collagen I molecules with an atomic force microscope. Biomechistry 38, 9956–9963.

Lo, C.-M., Wang, H.-B., Dembo, M., Wang, Y., 2000. Cell movement is guided by the rigidity of the substrate. Biophys. J. 79, 144–152.

Meshel, A. S., Wei, Q., Adelstein, R. S., Sheetz, M. P., 2005. Basic mechanism of three–dimensional collagen fibre transport by fibroblasts. Nature Cell Biol. 7, 157–164.

Ohsumi, T. K., Flaherty, J. E., Evans, M. C., Barocas, V. H., 2008. Three-dimensional simulation of anisotropic cell-driven collagen gel compaction. Biomech. Model. Mechanobio. 7, 53–62.

Pedersen, J. A., Swartz, M. A., 2005. Mechanobiology in the third dimension. Ann. Biomed. Eng. 33, 1469–1490.

Poole, K., Khairy, K., Friedrichs, J., Franz, C., Cisneros, D. A., Howards, J., Mueller, D., 2005. Molecular–scale topographic cues induce the orientation and directional movement of fibroblasts on two–dimensional collagen surfaces. J. Mol. Biol. 349, 380–386.

Rodriguez, E. K., Hoger, A., McCulloch, A. D., 1994. Stress-dependent finite growth in soft elastic tissues. J. Biomech. 27, 455–467.

Soulhat, J., Buschmann, M. D., Shirazi-Adl, A., 1999. A fibril–network–reinforced biphasic model of cartilage in unconfined compression. J. Biomech. Eng. 121, 340–347.

Thomopoulos, S., Fomovsky, G. M., Chandran, P. L., , Holmes, J. W., 2007. Collagen fiber alignment does not explain mechanical anisotropy in fibroblast populated collagen gels. J. Biomech. Eng. 129, 642–650.

Thomopoulos, S., Fomovsky, G. M., Holmes, J. W., 2005. The development of structural and mechanical anisotropy in fibroblast populated collagen gels. J. Biomech. Eng. 127, 742–750.

Tóth, M., Násady, G. L., Nyáry, I., Kerényi, T., Orosz, M., Molnárka, G., Monos, E., 1998. Sterically inhomogenous viscoelastic behavior of human saccular cerebral aneurysms. J. Vasc. Res. 35, 345–355.

Watton, P. N., Hill, N. A., Heil, M., 2004. A mathematical model for the growth of the abdominal aortic aneurysm. Biomech. Model. Mechanobio. 3, 98–113.

Zhu, C., Bao, G., Wang, N., 2000. Cell mechanics: Mechanical response, cell adhesion, and molecular deformation. Ann. Rev. Biomed. Eng. 2, 189–226.